Ichnology, Sedimentology and Paleontology of Eocene Calcareous Paleosols From a Palustrine Sequence, Argentina

RICARDO N. MELCHOR
CONICET & Universidad Nacional de La Pampa, Av. Uruguay 151, 6300 Santa Rosa, La Pampa, Argentina

JORGE F. GENISE
CONICET & Departamento de Icnología, Museo Paleontológico "Egidio Feruglio", Av. Fontana 140, 9100 Trelew, Chubut, Argentina

SERGIO E. MIQUEL
CONICET & Museo Argentino de Ciencias Naturales "Bernardino Rivadavia", Av. Ángel Gallardo 470, 1405 Buenos Aires, Argentina

PALAIOS, 2002, V. 17, p. 16–35

Integrated analysis of the ichnology, sedimentology, geochemistry, and fossil content of three trace fossil-bearing calcareous paleosols from the early Eocene Gran Salitral Formation is used to reconstruct the detailed paleoenvironmental and paleoecological setting of this insect-dominated ichnofossil association. This continental sequence, located in southwestern La Pampa province (Argentina), is composed of palustrine marls and minor lacustrine mudstones and sandstones arranged in shallowing-upward cycles. The ichnologic association is the first comprehensively described from a palustrine sequence and could be used for future comparisons with other similar assemblages. The ichnofauna is dominated by bee cells, Celliforma germanica, C. roselli, *and* Rosellichnus *isp.;* Teisseirei barattinia, *an insect trace fossil that is redescribed and recorded for the first time outside its type locality;* Taenidium barretti*; and* Skolithos linearis. *The ichnologic association also includes ovoid structures, ornamented burrow fillings, and plant trace fossils (rootlets, rhizoliths, and a tree / shrub stump). Abundant freshwater (*Pomacea *sp.) and terrestrial gastropods (*Plagiodontes *spp.,* Bostryx *sp., and* Bulimulus *sp.) are used to characterize the paleoenvironmental setting. The weakly developed paleosols are interpreted as Inceptisols, developed in a low-gradient lake margin periodically exposed to pedogenesis with low (probably saline) vegetation and sparse shrubs. They developed under a semi-arid and warm climate (mean annual temperature higher than 20°C). Short saline / alkaline conditions were prevalent during lake lowstands, accompanied by incipient karst development. The association of trace fossils is attributed provisionally to the* Coprinisphaera *ichnofacies, although its distinctive features and recurrence in time and space may deserve recognition as a separate ichnofacies.*

INTRODUCTION

Calcareous paleosols bearing insect trace fossils have been recorded from several localities in the world. Frenguelli (1930) was the first to mention a fossil insect nest occurring in a calcareous paleosol, later assigned to the Paleocene (Martínez et al., 1997). Other records were reported by Retallack (1984) from the Oligocene of the USA and by Thackray (1994) from the Miocene of Kenya. These paleosols share a similar paleontological content: terrestrial snails, hackberry endocarps, fossil bee cells, and other undetermined invertebrate and plant traces.

This paper documents early Eocene calcareous paleosols occurring in a palustrine sequence, that bear a similar association of continental snails, fossil bee cells, and other insect trace fossils (Fig. 1A, B). Palustrine sequences commonly are bioturbated (e.g., Platt and Wright, 1992), but no detailed description of their trace fossil content is known, to date, except for the recent report of Edwards et al. (1998). Ichnofossils and gastropods are analyzed in the framework of a detailed description of the trace-bearing paleosols, including field logging, micromorphology, x-ray diffractometry, major oxides ratios, and stable isotope geochemistry. These analyses have permitted detailed paleoenvironmental reconstruction and calibration of the environmental and ecological parameters of this community. In this context, this particular insect-dominated ichnologic assemblage may be used as a template for comparison with future ichnological/paleoecological studies of semiarid wetland environments. Furthermore, considering its recurrence in time and space (Paleocene of Uruguay, Oligocene of USA, Miocene of Kenya, and Eocene of Argentina), this association in calcareous paleosols is considered a potential continental ichnofacies, as previously suggested by Genise et al. (2000).

GEOLOGICAL SETTING

The surface geology of the area bordering the large depression of Gran Salitral (meaning great salt lake, Fig. 1C) is composed of Permo-Triassic to Recent units (Linares et al., 1980; Melchor and Casadío, 2000). Fault blocks of volcanic rocks assigned to the Choiyoi volcanism (Choique Mahuida Formation) are overlain by early Danian shallow-marine carbonates (Roca Formation), early Eocene shallow-lacustrine deposits with paleosols (Gran Salitral Formation), and Eocene shallow- to deep-lacustrine sedi-

0883-1351/01/0017-016/$3.00

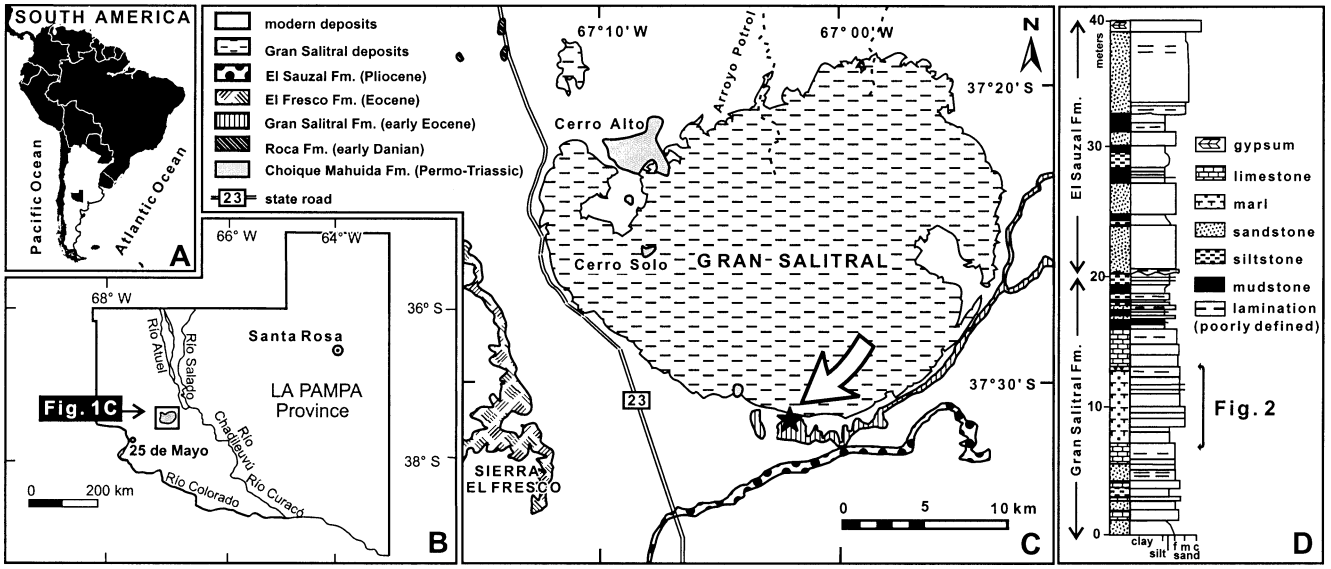

FIGURE 1—Location map and lithologic section of the Gran Salitral Formation. (A, B) Position of La Pampa province in South America and location of the study area. (C) Geologic map of the Gran Salitral depression area (modified from Melchor and Casadío, 2000). Black star (arrowed) indicates the study locality (37° 32′ 49″ S; 67° 04′ 14″ W). (D) Composite lithologic log of the Gran Salitral and El Sauzal formations at the study locality. The interval represented in Figure 2 is bracketed.

mentary rocks (El Fresco Formation). This succession is capped unconformably by Pliocene (?) sandstones and calcrete included in the El Sauzal Formation (Fig. 1D), which are overlain by modern deposits.

The Gran Salitral Formation is exposed in a *ca.* 40-m-high mesa-like feature on the southeast and east margins of the Gran Salitral depression (Fig. 1D). This unit was proposed by Melchor and Casadío (2000) to include continental lithic arenites, siltstones, mudstones, and limestones of probable Miocene age that crop out in the westernmost area of the geologic map 3766-III "La Reforma" (southwest La Pampa province). Further mapping and additional geochronologic information (Melchor, unpublished) indicate that this unit is restricted to outcrops on the margin of the Gran Salitral depression and is early Eocene in age (Fig. 1C).

METHODS

Thin sections for micromorphology were prepared thinner than usual (~20 μm) and the descriptive terminology of Bullock et al. (1985) was followed. To estimate modal composition of the paleosols, a total of 500 points per thin section were counted. Rock color was measured dry with a Rock Color Chart (Goddard et al., 1980).

A total of 33 stable isotopes analyses (C and O) on 7 bulk carbonate samples, including one to three replicates to evaluate sample heterogeneity, were performed at the University of Michigan Stable Isotope Laboratory. A polished chip of sample 259A was drilled in spar-filled fenestrae and micritic matrix to compare its isotopic composition. Powdered carbonate samples weighting a minimum of 10 milligrams were placed in stainless steel boats and heated at 380 °C *in vacuo* for one hour to remove volatiles. Samples then were placed in individual borosilicate reaction vessels and reacted at 76 ± 2 °C with 3 drops of anhydrous phosphoric acid for 8 minutes in a Finnigan Kiel preparation device coupled directly to the inlet of a Finnigan MAT 251 triple collector isotope-ratio mass spectrometer. Isotopic enrichments are corrected for acid fractionation and ^{17}O contribution by calibration to a best-fit regression line defined by two NBS standards, NBS-18 and NBS 19. Data are reported in ‰ notation relative to VPDB (Vienna Pee Dee Belemnite). At least six powdered carbonate standards were reacted and analyzed daily, bracketing the sample suite at the beginning, middle, and end of the day's run. Measured precision is maintained at better than 0.1 ‰ for both carbon-and-oxygen isotope compositions.

Major element and some trace elements of bulk marl and tuff samples were analyzed at Activation Laboratories Inc. (Canada) by Inductively Coupled Plasma mass spectrometry. FeO was analyzed by titration and CO_2 by infrared. Detection limits were 0.01%, except for FeO (0.1%) and CO_2 (0.05%). Due to the low-Mg content of calcite (as revealed by x-ray diffractometry), the total carbonate content in Figure 2 was estimated by considering all CO_2 content (Appendix 1) as coming from $CaCO_3$. The guidelines of Retallack (1990a) were followed in the calculation and interpretation of molecular weathering ratios. The chemical index of alteration (CIA) was calculated as (Nesbitt and Young, 1982; Fedo et al., 1995):

$$CIA = Al_2O_3/[Al_2O_3+K_2O+Na_2O+CaO^*]$$

where CaO^* = mol CaO − mol CO_2 − (0.5 x mol CO_2) − (10/3 x mol P_2O_5).

The mineralogy of seven samples was identified from x-ray diffractometer patterns recorded on whole-rock powder, for the angular range 2°–60° 2θ, with Cu Kα radiation, at 1° 2θ / minute, 35 Kv and 15 mA, on a Rigaku Denki DMAX-IIIC diffractometer from the Universidad Nacional del Sur, Bahía Blanca, Argentina.

Institutional abbreviations used in this paper are as follows: MFLR: Museo "Francisco Lucas Roselli" (Nueva Pal-

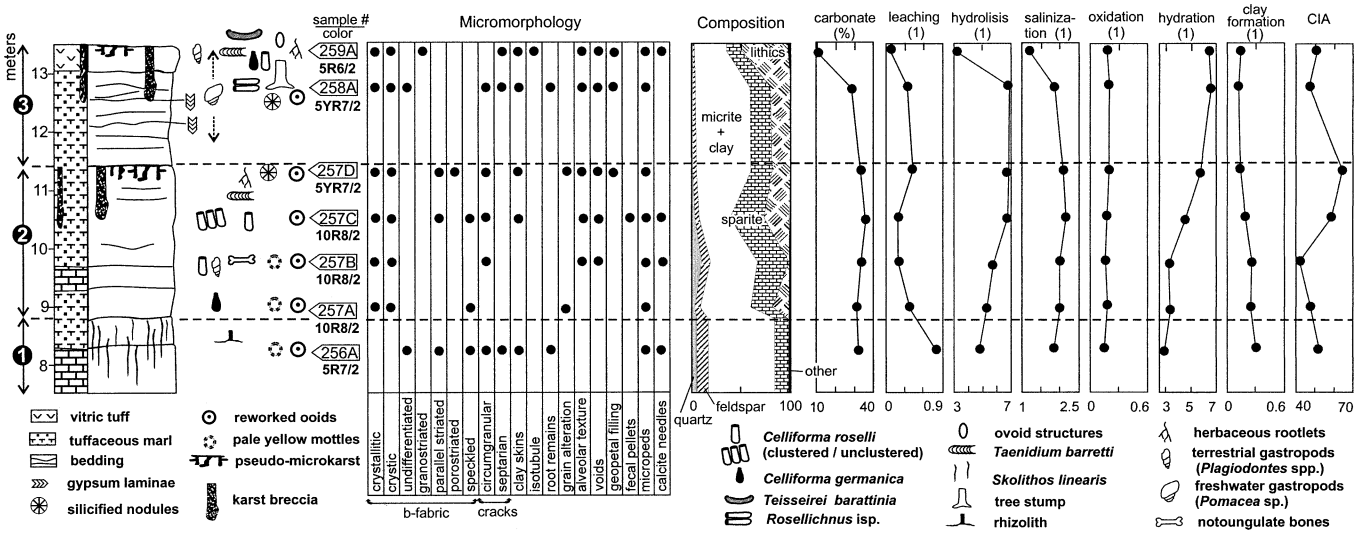

FIGURE 2—Paleosol details including lithology, sedimentary structures, trace fossils, body fossils, sample position, dry color, micromorphology, modal composition, calcium carbonate content, molecular weathering ratios, and chemical index of alteration (CIA). 1, 2, 3 indicate paleosols 1, 2, and 3, respectively. (1) Molecular weathering ratio formulae: Leaching = Ba/Sr, hydrolysis = $(CaO + MgO + K_2O + Na_2O) / Al_2O_3$, salinization = Na_2O/K_2O, oxidation = $(Fe_2O_3 + FeO + MnO) / Al_2O_3$, hydration = $SiO_2 / (Fe_2O_3 + Al_2O_3)$, clay formation = Al_2O_3 / SiO_2.

mira, Uruguay); MACN-LI: Museo Argentino de Ciencias Naturales "Bernardino Rivadavia," Laboratorio de Icnología (Buenos Aires, Argentina); GHUNLPam: Cátedra de Geología Histórica, Universidad Nacional de La Pampa (Santa Rosa, La Pampa, Argentina).

RESULTS

Sedimentology

Dominant lithologies of the Gran Salitral Formation are grayish orange pink (5YR7/2) to pale-red (10R6/2) marls with common pedogenic modification (as described below), limestones, red laminated mudstones, fine-grained sandstones, and vitric tuffs (Fig. 1D). The succession at the locality studied begins with 6.6 m of pale orange (10YR7/2) to grayish orange pink (5YR7/2) limestones interbedded with sandstones and minor siltstones (Fig. 1D). The overlying 9-m-thick section includes pedogenically modified tuffaceous marl, massive limestones, and discrete vitric tuff beds (Figs. 1D, 2); these are arranged in three shallowing-upward cycles (Fig. 2). The lower half of this interval is mostly structureless or exhibits poorly defined bedding. The upper half, is characterized by laterally continuous 0.1–0.5-m-thick beds with undulating contacts (Fig. 3F). Carbonate content ranges from 11 to 36 % in volume and is represented mostly by micrite and minor sparry calcite (Fig. 2). The succession is capped by 1.5-m-to-4 m-thick laminated pale red (10R6/2) to grayish red (5R4/2) lacustrine mudstone with minor interbedded tuff, limestone, and sandstone.

Paleosol Description

Three conspicuous paleosols were recognized in the measured section of the Gran Salitral Formation (identified by numbers 1–3 in Fig. 2), mostly based on their field features. These paleosols are weakly developed (scale of Retallack, 1990a, p. 265), poorly horizonated, and show an upward trend toward slightly more developed soil features. Special attention was paid to this interval because of the occurrence of abundant insect trace fossils and gastropods, which are accompanied by other invertebrate ichnofossils, rhizoliths and root marks, and scarce vertebrate bones (probably a notoungulate; Tonni, pers. comm., 2000). Figure 2 summarizes macroscopic and micromorphologic attributes, as well as lithologic, petrographic, geochemical, ichnologic, and paleontologic data on these paleosols.

Macrofeatures

All paleosols mostly are developed on tuffaceous marl. Paleosol 1 (1.20 m thick) is composed of grayish pink (5R7/2) massive marl with common, distinct, fine pale yellow (10Y8/2) mottles (descriptive terminology after Retallack, 1990a) and is devoid of insect trace fossils and gastropods remains. A slight reddening is apparent toward the top of the soil profile, which is truncated erosively by the overlying bed. Its salient macroscopic feature is the abundance of vertical burrows (*Skolithos linearis*), which obliterates the original sedimentary fabric (Fig. 3A). This paleosol

→

FIGURE 3—Selected paleosol macrofeatures. (A) *Skolithos linearis* in paleosol 1 (hammer = 35 cm long). (B) Medium-sized rhizolith (see arrows) and *Skolithos* burrow (Sk) from top of paleosol 1 (scale in cm). (C) Dissolution pit filled with intraformational breccia near the top of paleosol 2. Notice abrupt truncation on top. (D) Tubular cavities, snails (s), and pseudo-microkarst (p), in the upper part of paleosol 3 (pen = 13 cm). (E) Polished slab of sample 259A from top of paleosol 3 showing incipient glaebule (g), fine tubular cavities (t), and spar filled fenestrae (f). (F) Close-up of the top of the section showing lenticular bedding and the uppermost tuff bed (t). Hammer head is 15 cm long.

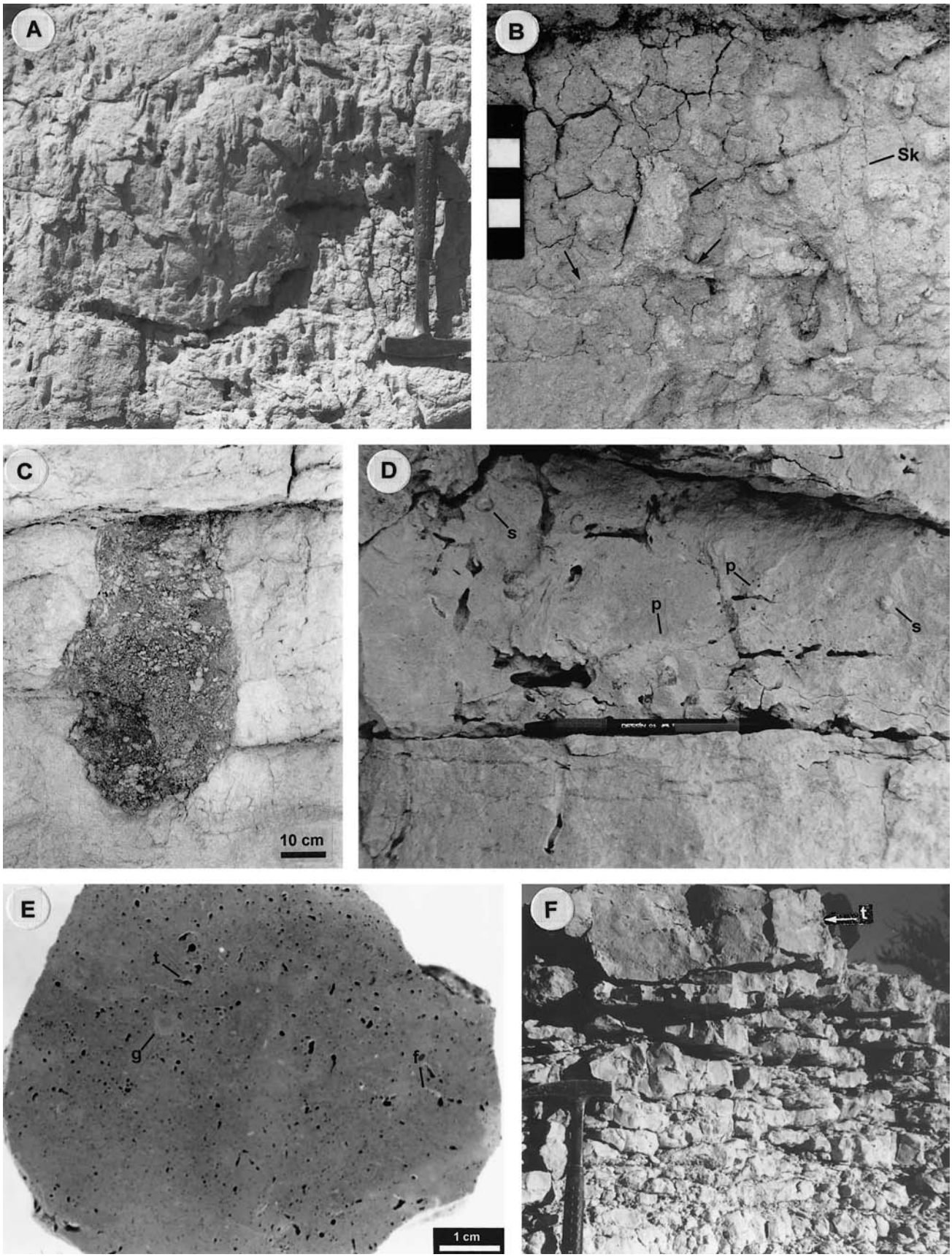
A
B
Sk
C
10 cm
D
s
p
p
s
E
t
g
f
1 cm
F
t

contains a few laterally spreading rhizoliths of medium size in its upper part (Fig. 3B).

Paleosol 2 (2.8 m thick) exhibits well-defined stratification in the lower half and is massive in the rest of the profile. Its color is very pale-orange (10YR8/2) with pale-yellow (10Y8/2) mottles that change to grayish orange pink (5YR7/2) in the upper half-meter (Fig. 2). Locally, paleokarst pits were observed in this and the overlying paleosol; some start in the upper third of paleosol 3 and penetrate down into the upper part of paleosol 2. These pits are vertical, cylindrical to funnel-shaped dissolution cavities (about 0.4 m wide and 0.5 m to *ca.* 3 m long) filled with sandstone-supported intraformational breccia (Figs. 2, 3C). Pseudo-microkarst (Freytet and Plaziat, 1982) was recognized in the upper half-meter of paleosols 2 and 3, as a horizontal to vertical, intricate network of tubular cavities (0.5–1 cm diameter) filled with calcareous sandstone. The most common ichnofossils in this paleosol are abundant bee cells, which are distributed throughout the soil profile, even in the lowermost 0.15 m, where evidence for pedogenesis is scarce. This ichnofauna is associated with terrestrial gastropods (*Plagiodontes* spp.) and scarce notoungulate remains.

Bedding in paleosol 3 (2.10 m thick) is well-defined and becomes thinner towards the top. The topmost meter is composed of lenticular laminae interbedded with millimeter-thick gypsum laminae; this is capped by a 0.35-m-thick ash-fall tuff (Fig. 2). The tuff bed is highly indurated and its color is slightly redder (pale red) than the underlying beds (grayish orange pink), which display nodular weathering. Planar and curved voids (terminology after Freytet and Plaziat, 1982), incipient glaebules (Fig. 3E), and interconnected tubular vugs (diameter less than 1 cm; see Fig. 3D) were identified in the upper 3 cm of this paleosol. Plant traces occur as common fine tubules (Fig. 3E) and a single tree or shrub stump cast is present.

Microfeatures

Main micromorphological attributes and compositional data are summarized in Figure 2. In paleosol 1, there are also thin clay coatings on skeletal grains and patchy development of angular blocky micropeds limited by carbonate veins (Fig. 4A).

In paleosols 2 and 3, there is an upward increase in the proportion of volcanic grains (Fig. 2). Subspherical and subangular, scattered calcareous ooids and oomolds are present in the entire profile of paleosol 2 and part of paleosol 3, although their abundance is less than 1% (Fig. 4B). Ooid maximum diameter ranges between 0.48 mm and 0.15 mm, averaging 0.28 mm. The best-preserved ooids exhibit a faint radial structure and commonly a micritized outer rim (Fig. 4B). Mostly micrite and clay minerals, in addition to minor opaque minerals, compose the groundmass of paleosol 2. Alveolar structure and sparite-filled fenestrae (Esteban and Klappa, 1983) are very rare at 1.8 m from the top of paleosol 2 an upward increase in abundance. Microlaminated clay fillings, geopetal fabrics, clay coatings (grain cutans), and probable fecal pellets were detected only in the uppermost meter of the profile (Fig. 2). The uppermost 30 cm of paleosol 2 shows a clotted-peloidal structure (Fig. 4D) in the sense of Armenteros and Daley (1998). Abundant sparitic cementation in localized areas transformed the rock into a diagenetic peloidal grainstone (Fig. 4E). Peloids (40 μm − 170 μm in diameter) are more or less differentiated from the homogeneous micritic matrix and usually are bound by a drusy sparite mosaic or veins. Probable silica nodules also were identified in the upper part of this paleosol.

In paleosol 3, groundmass composition, b-fabric, and clotted-peloidal structure are similar to that at the top of paleosol 2. The abundance of alveolar structure and clay coatings, along with geopetal fillings and fenestrae, are distinct micromorphological features of this paleosol (Fig. 5B, C, D). Fenestral cavities (up to 2 mm in diameter) are cemented by calcite crystal silt (below) and drusy sparite mosaic (above); a marginal, laminated micritic coating is locally present (Fig. 5D). Septarian and circumgranular cracks, pendant cement, and probable phytoliths also were identified sporadically. Clay coatings are more abundant in the uppermost part of paleosol 3 (reaching about 1% in volume). They coat terrigenous grains, peloids, and cavities; they are microlaminated and commonly show crescent morphology and cracks (Fig. 5C). In the middle part of paleosol 3, sparse silica nodules, up to 2.5 mm in diameter, were observed in thin section. They contain spherulites (about 1 mm in diameter) consisting of quartzine (length-slow chalcedony) and coarse granular calcite crystals (Fig. 5E).

Whole-Rock Chemistry

Major element data are tabulated in Appendix 1. All the major oxides except P_2O_5 and SiO_2 increase upward in paleosol 2. For paleosol 3, this vertical trend is different (essentially reflecting differences between the topmost tuff and the underlying tuffaceous marl); all oxides increase except for P_2O_5, Na_2O, CaO, and MnO, which are depleted near the upper part of the soil. The chemical data in Appendix 1 were used to estimate six molecular ratios (following Retallack, 1990a) that are displayed in Figure 2. The chemical index of alteration (CIA; Nesbitt and Young, 1982) ranges between 42 and 64, with the higher values corresponding to the upper part of the paleosols (Fig. 2). Gain and losses during soil formation were estimated using a sample of the base of paleosol 2 as possible parent material (sample 257A), and assuming TiO_2 as a stable constituent. This sample was chosen because of its very low CIA and preservation of primary sedimentary structures. Results of this procedure are plotted in Figure 6.

Stable Isotope Data

Analyses of C and O stable isotopes (n = 33) correspond to whole-rock powder, carbonate matrix, and sparry calcite from fenestrae (the two last components only for sample 259A). Results are tabulated in Appendix 2 and plotted in Figure 7. The carbonate phase analyzed is low-Mg calcite as inferred from x-ray diffractometry data.

Most of the data lie on an approximately linear trend in the negative $\delta^{13}C$, negative $\delta^{18}O$ quadrant, with spreads of $\delta^{13}C$ from −4‰ to −7‰ and of $\delta^{18}O$ from −3‰ to −6‰ (Fig. 7A). Whole rock values for paleosols 2 and 3 show limited variation ($\delta^{13}C$ = −5.65‰ to −4.52‰, $\delta^{18}O$ = −3.51‰ to −3.03‰), although there is a general upward trend to lighter values, especially for $\delta^{13}C$ (Fig. 7B). The

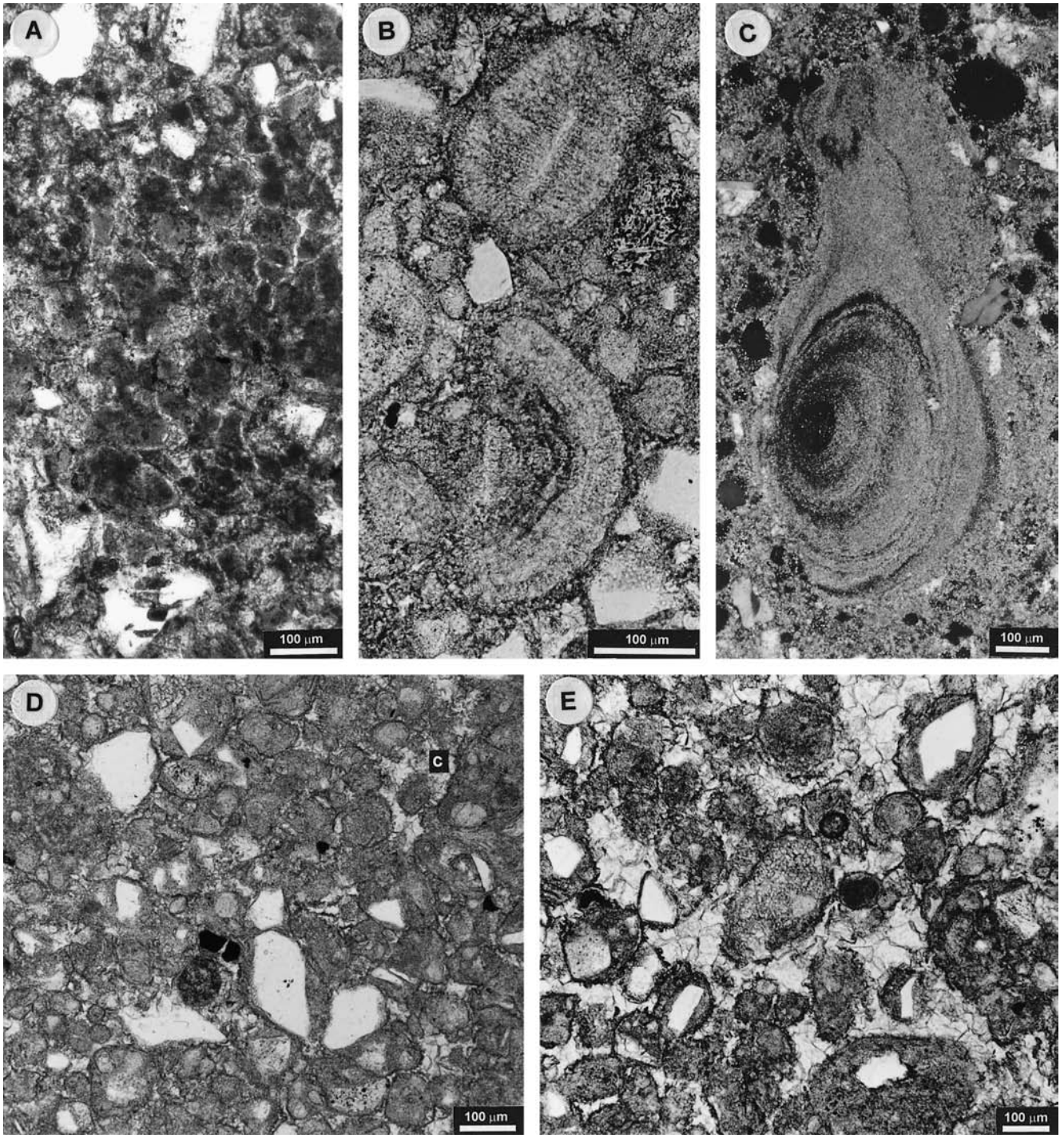

FIGURE 4—Photomicrographs of paleosols 1 and 2. (A) Localized development of blocky micropeds from paleosol 1 (sample 256A). (B) Complete (above) and subangular broken ooid (below) with planar nucleus (skeletal remain; sample 257C). (C) Laminated clay filling (sample 257D). (D) Clotted-peloidal fabric with abundant peloids and crystallitic b-fabric (c). Note that siliciclastic grains are included in some peloids (sample 257C). (E) Diagenetic grainstone composed of peloids and abundant drusy sparite (sample 257D). Photographs with ordinary light except for C (crossed nicols).

components analyzed separately in sample 259A display greater heterogeneity; the more enriched values approach the isotopic composition of the micritic matrix carbonate, and the more depleted values are closer to the composition of the sparry calcite of fenestrae (Fig. 7A). Intermediate values likely reflect different contributions of each component (matrix and spar).

X-ray Mineralogy

The dominant minerals identified by X-ray diffractometry in the seven samples analyzed are low-magnesium calcite, plagioclase feldspar, zeolites (in particular mordenite, phillipsite, and clinoptilolite), and quartz (Appendix 3). $MgCO_3$ content of calcite is usually 1–2%, although

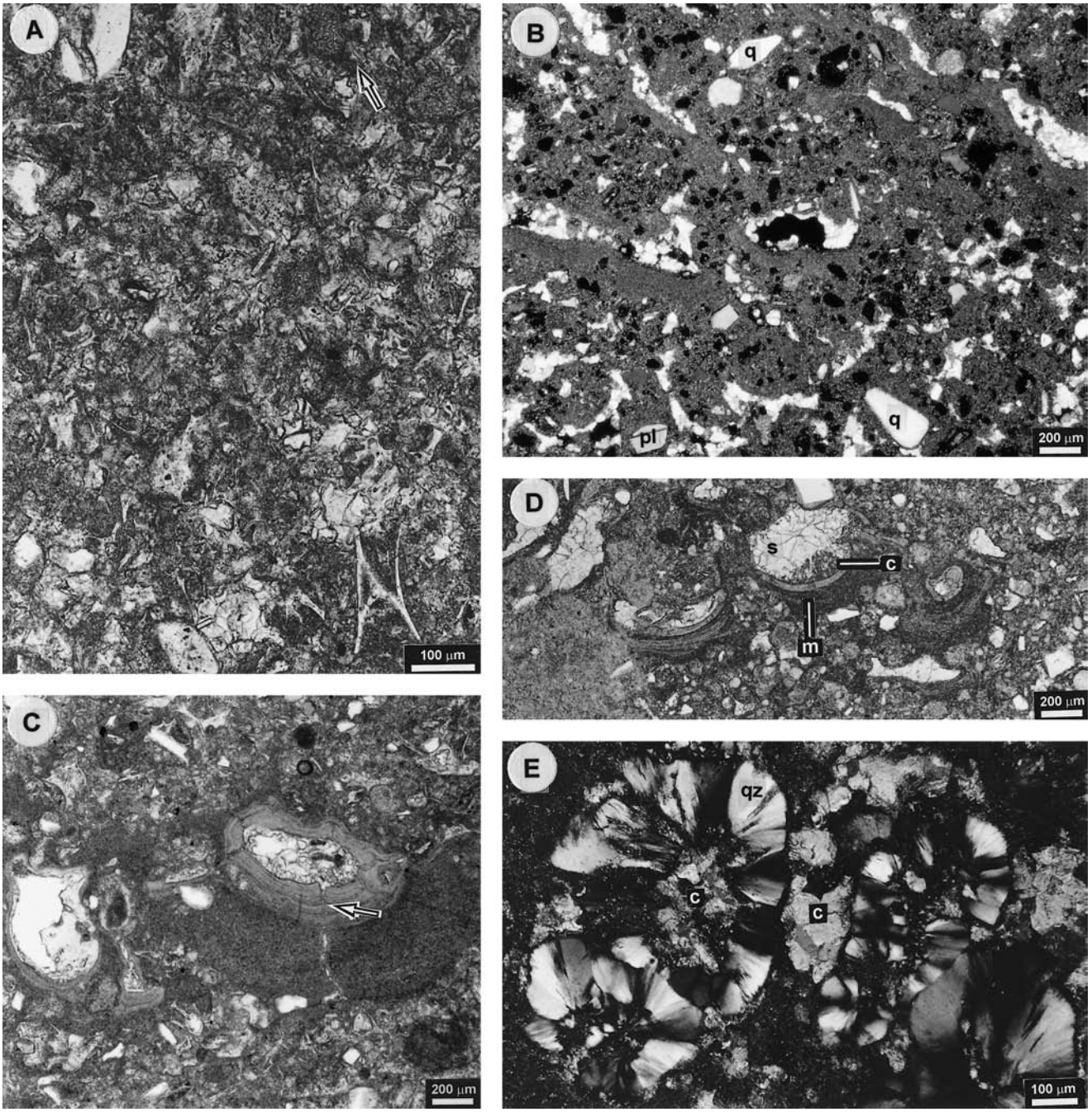

FIGURE 5—Photomicrographs of paleosol 3. (A) Microscopic view of the uppermost tuff bed within paleosol 3 showing abundant glass shards, micrite, and probable phytoliths, in addition to drusy calcite cementation and localized development of peloids (arrow; Sample 259A). (B) Fenestral and alveolar structures from sample 258A. pl = plagioclase, q = quartz. (C) Cavity with a complex, geopetal filling including micrite plus silt-sized siliciclastic grains (margin), microlaminated clays with quasi radial cracks (arrow), and drusy calcite (center; sample 259A). (D) Geopetal filling of cavities. Microlaminated micrite and clay with pendant geometry (m), crystal silt (c), and calcite spar (s). (E) Nodule composed by quartzine (qz) and calcite (c). Sample 258A. Photographs with ordinary light except for E (crossed nicols).

in a single sample it reaches about 3–4%. Other minerals recognized in minor amounts are K-feldspar and probable sepiolite. The presence of zeolites is important in the sequence (about 20% to 30% whole rock).

Trace Fossil Assemblage

The ichnologic assemblage is dominated by insect trace fossils (especially bee cells and chambers of uncertain origin), meniscate burrows, ornamented burrow fillings, ovoid structures, and plant ichnofossils (Figs. 2, 3A, B, E, 8–12). Bee cells are so abundant in paleosol 2 that, when broken with a hammer, almost every fist-sized piece of rock bears at least one cell.

Three ichnotaxa of bee cells have been distinguished: *Celliforma germanica*, *Celliforma roselli*, and *Rosellichnus* isp. The *Celliforma* specimens include isolated cells and

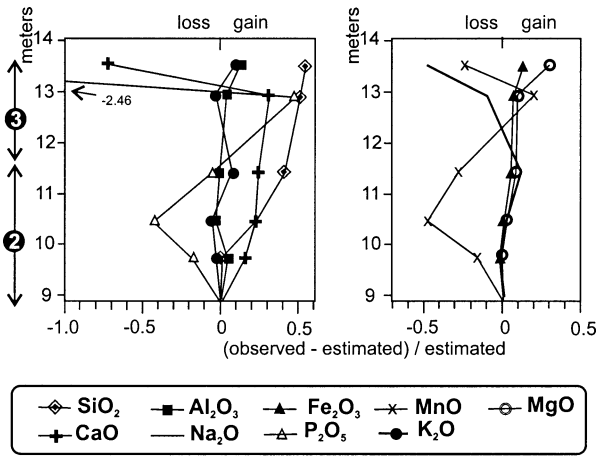

FIGURE 6—Estimated elemental gains and losses during soil formation. The plotted ratio measures the degree of departure from the estimated concentration of each element (see text for explanation). Changes in paleosol bulk density were not measured. Data from Appendix 1.

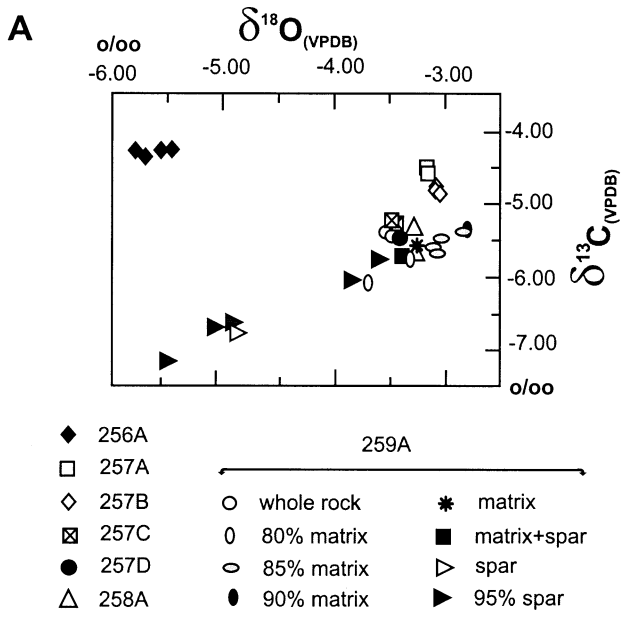

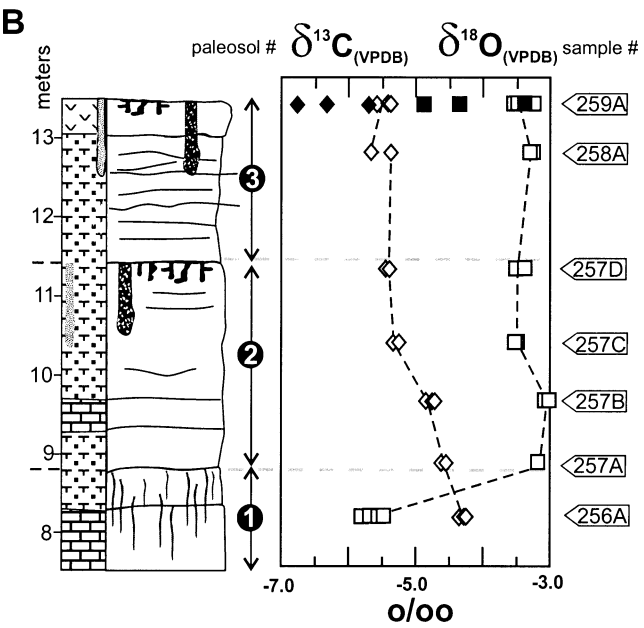

FIGURE 7—Carbon and oxygen isotopic data (note that symbols used in A are not equivalent to those used in B). (A) Cross-plot of $\delta^{13}C$ and $\delta^{18}O$ (PDB) for the different phases analyzed by stable isotope geochemistry (see text for discussion). (B) Vertical distribution of $\delta^{13}C$ and $\delta^{18}O$ (PDB). Open symbols: whole-rock data; solid symbols: material drilled on polished slab (sample 259A). See Figure 2 for additional references. Data from Appendix 2.

cells arranged in rows, while *Rosellichnus* is characterized by clusters of cells (cf. Genise, 2001). *Celliforma germanica* (Figs. 8A, B, C, 9A) includes elongated, tear-shaped cells having rounded bottoms and flat tops, which are preceded by a constriction or neck. In some specimens, the neck may be masked by a ring of matrix (i.e., Frenguelli, 1938a; fig. 3). The length of the cells ranges from 14 mm to 20 mm and the maximum diameter from 4 mm to 7 mm (mean = 6 mm, n = 35). Their orientation in the paleosols is subvertical to subhorizontal. Cells may occur as isolated traces or grouped in sloping rows of two to four cells (Fig. 9A). Two tiered rows of cells were observed. In one case, the bottom of a single cell was in contact with the top of the third cell of a row of three. In the other case, a row of two cells was separated by a short distance from a row of four. Rows of cells attached to one side of a tunnel are common in the nests of many digging bees. On the other hand, cell clusters composed of cells arranged simultaneously in rows and in end-to-end series are unknown from modern nests, suggesting that this tiered arrangement resulted, more likely, from the close construction of end-to-end series of cells at the distal extremes of independent, lateral tunnels excavated in close proximity. Cells having necks and arranged in an end-to-end design are common in nests of species of the Agapostemonini (Roberts, 1969) in which cells may be so densely grouped that they may look like tiered series as those described herein (e.g., Abrams and Eickwort, 1980). Specimens described by Schütze (1907) and Frenguelli (1938a), and some of those described by Frenguelli (1930, 1938b) and Martínez et al. (1997; *Celliforma* isp. A), belong also to *C. germanica* and occur in calcareous paleosols.

Celliforma roselli (Figs. 8D, E, 9B) comprises cylindrical to barrel-shaped, stout cells having rounded bottoms and flat or conical tops and lacking any other distinctive feature. The length of the collected cells ranges from 20 to 39 mm, but most of these specimens were broken, precluding the proper estimate of the mean value. The largest measured specimen is 39 mm (GHUNLPam 12474; Fig. 8E) and the second largest (34.5 mm) known is that collected by Frenguelli (1938b, plate VII, fig. 9). The length of the remaining three complete specimens ranges from 29 to 31 mm. The maximum diameter of the longest cell (GHUNLPam 12474) was 18 mm. The maximum diameter of the remaining cells (including those described by Frenguelli) ranges from 11 to 15 mm (mean = 13.28 mm, n = 16). Disposition of the cells in the paleosol was oblique to subvertical. Cells occur mostly as isolated traces but a group arranged in a row of six cells was also collected (Fig. 9B). Diameter of these cells is 11 mm and, in some of them,

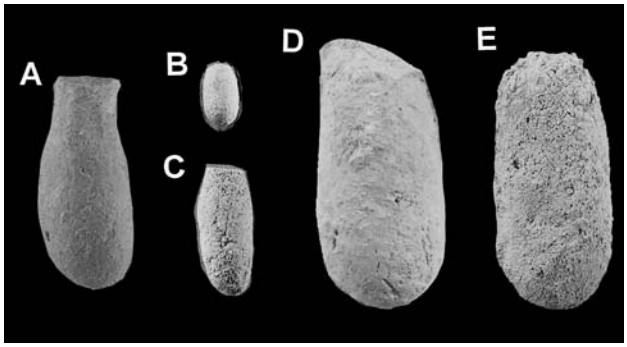

FIGURE 8—Selected specimens of *Celliforma germanica* (A, B, C) and *Celliforma roselli* (D, E). (A) MACN-LI 1314, X 1.6. (B) GHUNLPam 12465, X 0.95. (C) GHUNLPam 12460, X 0.9. (D) GHUNLPam 12464–3, X 1.0. (E) GHUNLPam 12474, X 0.8.

it was possible to recognize remains of a thin, discrete wall. Some of the fossil cells mentioned by Frenguelli (1930, 1938b) and by Martínez et al. (1997; *Celliforma* isp. B) also belong to *C. roselli* and occur in calcareous paleosols.

Rosellichnus isp. (Fig. 10) is composed by cells disposed in two rows of three and two cells, respectively. Cell diameter is 7 mm and cell length ranges from 21 to 25 mm. However, cell length may be overestimated because of the presence of a matrix hood at the tops. Isolated cells are in all aspects identical to *Celliforma germanica*, suggesting that at least some of them or those arranged in rows probably represent the first instars of the cluster construction. Thus, there is a high probability that the same trace maker constructed at least part of *Celliforma germanica* and

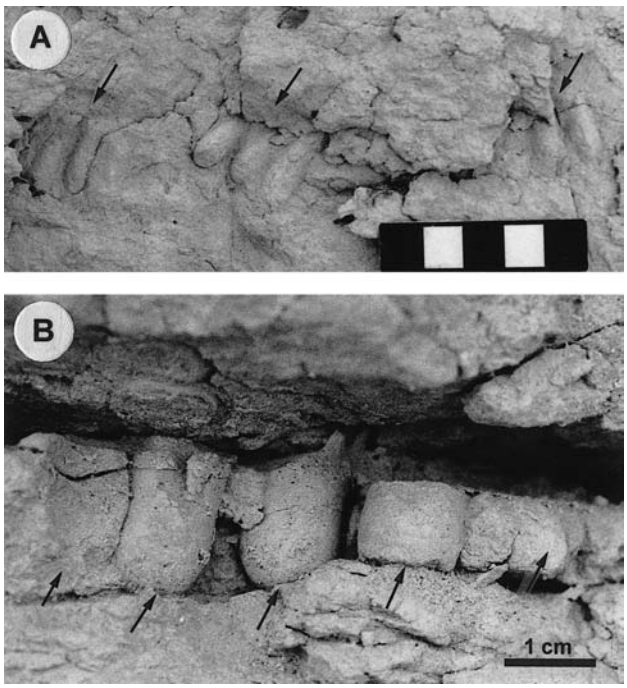

FIGURE 9—Field photographs of groups of *Celliforma* cells from paleosol 2. (A) Groups of two and three cells of *C. germanica* in sloping rows. Scale divisions = 1 cm. (B) Close-up of row of six cells of *C. roselli* (individual cells arrowed). Only five cells are shown.

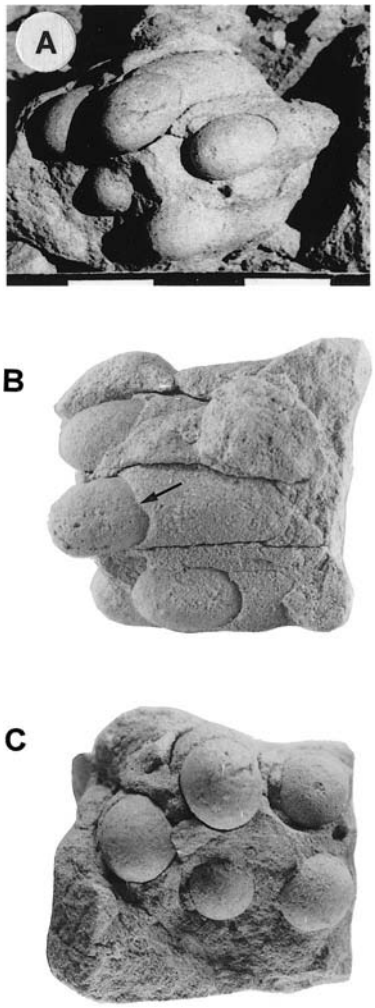

FIGURE 10—*Rosellichnus* isp. (A) Oblique field photograph of cluster (scale divisions on bottom = 1 cm). (B) View of cluster from above showing overall geometry and discrete wall indicated by arrow (X 1.1). (C) View of the rounded ends of cells (X 1.2). Notice the presence of matrix around cells. Specimen MACN-LI 1316.

Rosellichnus isp. In contrast with the described ichnospecies, *R. arabicus* and *R. patagonicus*, of uncertain origin, *Rosellichnus* isp. closely resemble in morphology, size, and thin cell walls the augochlorine clusters.

Teisseirei barattinia (Fig. 12A, B, C, D, E, I), another insect ichnotaxon (although of uncertain origin), which is abundant and restricted to the top of paleosol 3. *Teisseirei barattinia* is redescribed herein on the basis of abundant material collected in La Pampa (this study), Colón (also from Argentina), and many localities in Uruguay (Appendix 4). Other trace fossils of probable insect affinity are "ovoid structures" (Fig. 12G, H), that frequently have been interpreted as wasp cocoons (e.g., Thackray, 1994; Bown et al., 1997). They display an ovoid outline, having rounded extremes (length: 14–17 mm, width: 8 mm).

Meniscate burrows occur associated stratigraphically with *T. barattinia* (Fig. 2) and are assigned to *Taenidium barretti* (Fig. 11). This ichnotaxon includes slightly curved, unwalled, subhorizontal burrows of uniform diameter (8–9 mm) with thin, deeply arcuate menisci.

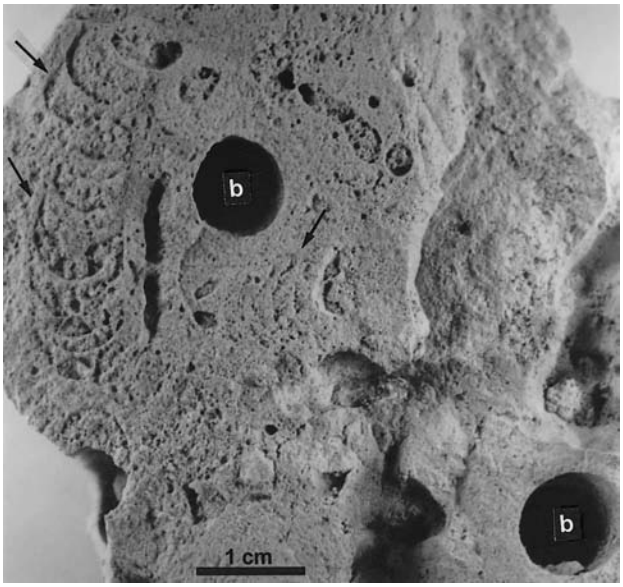

FIGURE 11—*Taenidium barretti* from top of paleosol 3 (GHUNLPam 12486). Three subhorizontal specimens are shown (arrowed) along with a transverse section of probable empty bee cells (b).

Two additional types of burrow were recognized: *Skolithos linearis* (Fig. 3A) and ornamented burrow fillings (Fig. 12F). *Skolithos linearis* comprises dominantly vertical, straight to slightly curved burrows with subcircular cross-section (burrow diameter ranges from 7.5 mm to 11.0 mm), smooth boundaries, and no wall. They are very abundant in paleosol 1 (Figs. 2, 3). Ornamented burrow fillings are internally massive and display a distinct scaly surface morphology, that is similar to the scratches observed in the best preserved specimens of *Teisseirei* (compare Fig. 12F and 12I).

Three different types of plant ichnofossils were identified: a single tree / shrub stump cast in paleosol 3 (about 0.15 m in diameter), medium sized rhizoliths (2 cm in diameter) with laterally spreading root molds on top of paleosol 1 (Fig. 3B), and common fine rootlets (Fig. 3E) mainly in the upper part of paleosols 2 and 3 (see also Fig. 2). Rootlets are open or spar-filled, tubular cavities, up to 2 mm in diameter, which are abundant in the upper part of paleosols 2 and 3 (Figs. 2, 3E).

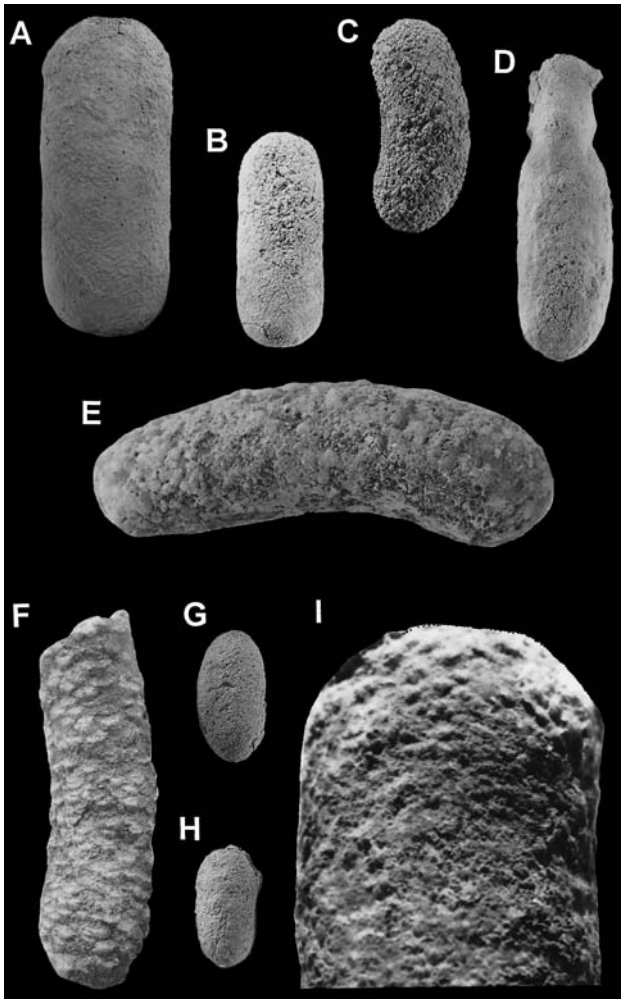

FIGURE 12—*Teisseirei barattinia* (A-E, I) and other trace fossils (F-H). All photographs of *Teisseirei barattinia* taken with the concave side up except for E. See complete description in Appendix 4. (A) Largest collected specimen, GHUNLPam 12462–1, X 0.8. (B) Medium-sized specimen, GHUNLPam 12473–5, X 0.8. (C) Laterally curved specimen of *T. barattinia*, GHUNLPam 12478–5, X 0.7. (D) *T. barattinia* with antechamber, MACN-LI 1309, X 0.7. (E) Lateral view of *T. barattinia*, GHUNLPam 12462–2. (F) Ornamented burrow filling with scaly surficial texture, GHUNLPam 12487, X 0.9. (G, H) Ovoid structures, GHUNLPam 12475–1/2, X 1.05. (I) Detail of the surface ornamentation in *Teisseirei barattinia* (MACN-LI 1308), X 1.6.

Gastropod Association

The collected material, largely preserved as internal molds, comprises both freshwater and terrestrial gastropods whose stratigraphic distribution is indicated in Figure 2. In the upper part of paleosol 3, terrestrial snails lay with their largest axis subhorizontal and with the aperture facing down, which is similar to the usual position during life. Terrestrial gastropods found *in situ* are restricted to the upper part of paleosol 3 (associated with freshwater gastropods) and in the lower part of paleosol 2.

The gastropod association includes numerous specimens of the freshwater snail *Pomacea* sp. (Fig. 13A) and three taxa of terrestrial snails, including *Plagiodontes* spp. (Figs. 13C, D) and scarce remains of *Bostryx* sp. (Fig. 13B) and *Bulimulus* sp. (Fig. 13E). A detailed taxonomic treatment of this fauna will be the focus of an additional contribution (Miquel, in prep.). In Argentina, the species of the Ampullariidae (which includes *Pomacea* sp.) inhabit subtropical to temperate areas up to 38° S. The Ampullariidae have branchia and lungs, preferring quiet and clear bodies of water, rivers, as well as temporary and permanent ponds. They also can withstand periods of desiccation and can live in waters of various salinities (Castellanos and Fernández, 1976). The modern species of *Plagiodontes* inhabit principally semiarid areas of northern and central Argentina, reaching the Tandilia-Ventania mountain systems (~ 38° S) in Buenos Aires province (Parodiz, 1939; Fernández, 1973). Similarly, the modern species of *Bulimulus* that closely resemble the fossil material is found in the semiarid Monte region of Argentina (Cabrera and Willink, 1973).

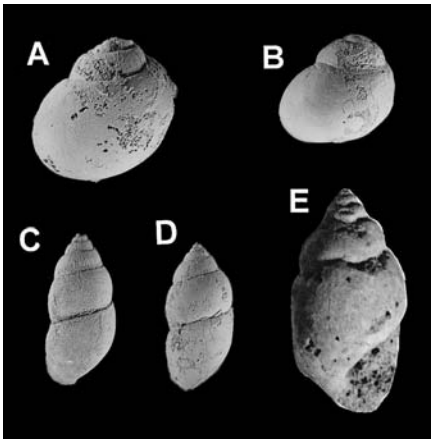

FIGURE 13—Freshwater and terrestrial gastropods. (A) *Pomacea* sp., GHUNLPam 12467–5, X 0.7. (B) *Bostryx* sp., GHUNLPam 12463–2, X 0.7. (C) *Plagiodontes* sp., GHUNLPam 12470–10, X 0.8. (D) *Plagiodontes* sp. MACN-LI 1330, X 0.65. (E) *Bulimulus* sp., MACN-LI 1332, X 1.5.

DISCUSSION

Table 1 summarizes essential descriptive and interpretative characteristics on the ichnology, sedimentology, and paleontology of the studied Eocene continental succession. Each of these are discussed below.

Paleoenvironmental Setting

The sequence is interpreted as a palustrine carbonate deposit (mostly pedogenically modified lacustrine marlstones) in the sense of Freytet (1973, 1984), Freytet and Plaziat (1982), and Platt (1989). Palustrine facies are typical of low-gradient, shallow freshwater environments in warm climates with reduced clastic supply (Platt and Wright, 1992). Palustrine carbonates have received increased attention recently and detailed descriptions were published by Esteban and Klappa (1983), Alonso-Zarza et al. (1992), Platt and Wright (1992), and Armenteros and Daley (1998).

The main palustrine features found in the Gran Salitral marls include: shallow water lithofacies; shallowing-upward cycles containing water-lain structures capped by paleosols; an association of freshwater and terrestrial gastropods, rhizoliths, root tubules; "grainification" (Alonso-Zarza et al., 1992); "pseudo-microkarst" (Freytet and Plaziat, 1982); and clotted-peloidal microstructures (Armenteros and Daley, 1998). The Gran Salitral palustrine facies are interpreted as having been deposited in a low-gradient lake-margin setting (cf. Freytet and Plaziat, 1982; Platt, 1989; Platt and Wright, 1991) subjected to repeated desiccation and flooding in response to water-level fluctuations. These palustrine deposits are closer to the semi-arid type distinguished by Platt and Wright (1992), because most cycles commence with horizons preserving freshwater fauna but cycle tops contain minor evaporites, terrestrial and freshwater gastropods, and evidence of desiccation. In addition to sedimentary features, a subaqueous origin for the parent material of paleosols 2 and 3 is reinforced by the presence of the freshwater gastropod genus *Pomacea*. The occurrence of *Pomacea* sp. and terrestrial snails (*Plagiodontes* spp.) on top of paleosol 3 also attest to the inferred subaqueous origin and later subaerial exposure of these sediments. Water-level changes exposed large littoral areas to pedogenesis, vadose diagenesis, and to colonization by burrowing animals (mostly insects) and sparse plants.

For the exposure surfaces described in this study, a first approximation to the mean number of days per year that the ground surface would have been covered with water, can be made by comparison with the exposure index for freshwater palustrine environments of Platt and Wright (1992). It is likely that paleosols 2 and 3 were emergent for most of the year, being covered with water for about 30 days per year (cf. fig. 8 of Platt and Wright, 1992). Probable hydromorphic features (mottling, laterally spreading rhizoliths) and absence of bee cells in paleosol 1 might indicate a longer flooding period over the course of its development.

Clotted-peloidal microstructure usually is interpreted as the result of repeated wetting and drying of lacustrine carbonate mud and likely formed via the following se-

TABLE 1—Key sedimentologic, ichnologic and paleoecologic features of the Gran Salitral palustrine sequence.

Lithology and paleoenvironmental setting
Tuffaceous marl with vadose textures and minor interbedded mudstones deposited in a shallow-lacustrine low-gradient margin. The lake experienced repeated hydrological restrictions.
Palustrine features
Shallow water facies, shallowing upward cycles with freshwater gastropods capped by paleosols and terrestrial gastropods, rhizoliths, grainification, pseudomicrokarst, clotted-peloidal microstructure, paleokarst pits.
Lake salinity
Longer freshwater periods during lake highstands (abundant freshwater gastropods, waterlain structures) punctuated by moderately saline/alkaline periods (evaporite nodules, gypsum laminae, radial aragonitic ooids) during lake lowstands. Lake margins were flooded about one month each year.
Paleosol characteristics
Poorly horizonated, weakly developed calcareous paleosols (Inceptisols), commonly with well-drained profile. Mildly saline/alkaline soil conditions favored zeolite authigenesis.
Ichnologic association
Bee cells (*Celliforma germanica, C. roselli, Roselichnus* isp.), other insect trace fossils (*Teisseirei barattinia,* ovoid structures), meniscate burrows (*Taenidium barretti*), dense concentration of *Skolithos linearis* burrows, unidentified burrow fillings, medium-sized rhizoliths, and tree or shrub stump.
Invertebrate trace makers
Insect dominated trace fossil association. Three or more species of sweat bees (tribes Augochlorini and Agapostemonini), other unidentified insects (producers of *Teisseirei* and ovoid structures), arthopods and/or annelids (*Skolithos*, *Taenidium*).
Gastropod association
Freshwater (*Pomacea* sp.) and terrestrial snails (*Plagiodontes* spp., *Bostryx* sp., *Bulimulus* sp.), the latter commonly restricted to paleosol tops.
Vegetation
Sparse low vegetation, probably saline shrubs and sage (features of plant ichnofossils, absence of dung-beetle trace fossils).
Climate
Semiarid (as suggested by sparse plant ichnofossils, abundant hymenopterous nests, gastropod association, paleokarst in calcareous paleosols, and scarce evaporites) and warm climate (mean annual temperature higher than 20°C).

quence: carbonate mud → nodulization (pelletization) → curved fissuring → coating of nodule (peloid) surfaces→ isolation of nodules (e.g., Freytet and Plaziat, 1982; Platt, 1989; Armenteros and Daley, 1998). Pseudo-microkarst structures, described and interpreted in detail by Freytet and Plaziat (1982) and Alonso-Zarza et al. (1992), are related to palustrine facies. They are considered as a pedogenic to very early diagenetic feature related to root penetration prior to lithification with minor participation of dissolution processes, distinguishing it from true karst. Other processes in pseudo-microkarst formation are desiccation, reworking, and microorganism activity (Alonso-Zarza et al., 1992). Paleokarst pits associated with the tops of paleosols 2 and 3 indicate a significant hiatus between successive lake-flooding events. Karst processes probably accompanied soil formation and were related to localized dissolution of the carbonate substrate, possibly enhanced by concentration of rainwater by tree stem-flow, in a similar way as proposed by Vanstone (1998).

Paleosol Interpretation

All described paleosols are similar to Inceptisols (Soil Survey Staff, 1999). They are distinguished from Entisols based on their finer grain size, composition of the parent material, and presence of a cambic horizon (denoted by limited accumulation of carbonate and clays in the uppermost preserved horizons). Other typical features for Inceptisols that could be identified or inferred include the abundance of easily weatherable volcanic material, development in young geomorphic surfaces, preference for depressions, and reduced rainfall (Foss et al., 1983; Fanning and Fanning, 1989; Buol et al., 1990). Limited salinization and absence of a calcic, petrocalcic, or gypsic horizon distinguishes these soils from Aridisols (cf. Fanning and Fanning, 1989). Furthermore, the relative abundance of volcaniclastic particles and zeolites is not considered significant enough to compare these paleosols with Andisols; the content of volcanic glass commonly is reduced, whereas Andisols typically support abundant vegetation and develop in areas of considerable rainfall (Soil Survey Staff, 1999).

Paleosol parent material was a carbonate-cemented, moderately zeolitized, secondary volcaniclastic deposit that have been reworked in a shallow lake. Carbonate participation was derived, in part, from clastic bedload (and probably eolian input) and from pedogenesis/early diagenesis. Molecular weathering ratios (Fig. 2) and the calculations of geochemical changes during soil formation (Fig. 6) indicate that these paleosols suffered little transformation during pedogenesis.

The uppermost part of paleosol 1 exhibits a darker color, rhizoliths, moderate leaching, and clay formation. The rest of the profile is compared to a C horizon with about 30% $CaCO_3$, and lacking any conspicuous segregation of carbonate. The total destruction of the sedimentary fabric in this interval was due chiefly to the activity of burrowing organisms that excavated vertical dwelling burrows (*Skolithos linearis*).

A cambic horizon (Bw) is identified within the upper meter of paleosol 2, especially based on the presence of massive structure and slightly darker color than the underlying soil profile. Due to the profusion of bee cells found in this horizon, bees likely played an important role in modification of the depositional fabric. Alveolar and fenestral structures were recorded as deep as 1.8 m below the top of paleosol 2, suggesting a probable maximum depth of root penetration. Very low CIA values (ranging from 41 to 47, see Fig. 2) for the underlying C horizon and the presence of relict layering and scarce microscopic pedofeatures are indicative of minor weathering and pedogenic modification. The upward decrease in the amount of P_2O_5 in the profiles for paleosols 2 and 3 is interpreted as recycling by plants and downward movement of percolating waters (Fenton, 1983).

In paleosol 3, an upper cambic horizon also can be discerned (Bw) on the basis of its color, structure (massive with abundant voids and rootlets), high induration, evidence for translocation of clays (clay coatings), and depletion of carbonates (Fig. 2). The lower horizon is labeled tentatively as Ck due to the sharp increase (11 to 29%) in calcium carbonate content compared with the overlying Bw horizon (Fig. 2). Paleosol 3 also is weakly developed, but the presence of a clear cambic horizon reflects a slightly more developed state. Paleokarst pits in paleosols 2 and 3 may suggest a slightly higher elevation during their development than in paleosol 1 (probably less than 3–5 m above lake level; see Platt and Wright, 1992).

The isotopic values for carbonates (Appendix 2) fall in the known range for calcretes (e.g., Talma and Netteberg, 1983; Rossinsky and Swart, 1993) and are close to available isotopic values for palustrine carbonates (Platt, 1989; Wright and Alonso-Zarza, 1992, Armenteros et al., 1992; Armenteros and Daley, 1998; Alonso-Zarza and Calvo, 2000; Tanner, 2000). A trend towards lighter isotopic values upsection is evident in Figure 7B, which parallels a concurrent higher degree of soil development inferred from macroscopic and micromorphological features. In particular, there is a slight decrease in $\delta^{13}C$ values and a subtle increase in $\delta^{18}O$ indicative of paleoexposure surfaces near the tops of paleosols 2 and 3 (Allan and Mathews, 1982; Goldstein, 1991). This is consistent with the values for the chemical index of alteration (CIA), which denotes an increase in chemical weathering toward the top of paleosols 2 and 3 (Fig. 2).

The light $\delta^{13}C$ values obtained are interpreted as reflecting modification due to influence of fractionated meteoric groundwater and isotopically light, soil-derived CO_2 in a near-surface, vadose diagenetic setting (Allan and Matthews, 1982; James and Choquette, 1990; Goldstein, 1991) or pedogenic setting (Beier, 1987; Cerling et al., 1988; Platt, 1989; Wright and Alonso-Zarza, 1992; Armenteros and Daley, 1998). The lightest $\delta^{13}C$ value (*ca.* −7.1 ‰) likely represents the closest approximation to the carbon isotopic composition of the soil-gas charged diagenetic fluids (cf. Cerling, 1984).

Lake and Soil Salinity

In the present study, the morphology of calcareous lacustrine ooids provides clues about lake salinity. The high percentage of syndepositionally broken ooids (Fig. 4B), faint radial microstructure in some ooids combined with small diameters (mean 0.28 mm), and evidence for ooid dissolution (oomolds) suggest that Gran Salitral ooids were originally radial aragonitic ooids associated with hy-

persaline shorelines similar to those of the Great Salt Lake (e.g., Halley, 1977) and the Late Triassic Mercia Mudstone Group at Clevedon, U.K. (Milroy and Wright, 2000). The presence of scarce silica nodules composed of quartzine are considered as a by-product of replacement of former gypsum or anhydrite nodules (Milliken, 1979; Hess, 1990). Sample 257D from the top of paleosol 2 contains about 3–4% $MgCO_3$, which might indicate a high-Mg calcite precursor. This mineral is most frequent in saline or brackish-water lakes (Eugster and Kelts, 1983). This evidence, along with the occurrence of abundant remains of freshwater gastropods (*Pomacea* sp.) throughout the section, would imply that the lake experienced short (hyper)saline periods (during lake draw down) within longer freshwater intervals. Despite evidence for moderate salinization, the stable isotopic data do not indicate fractionation associated with evaporative processes (Fig. 7A).

There is additional geochemical and mineralogical evidence that suggests partially saline and/or alkaline conditions during lake lowstands and soil development. The soda/potash ratio, which is close to 2 in the succession, indicates that pedogenesis was salt-influenced (Retallack, 1997). The increase in the ratio of bases to alumina (a proxy for the degree of hydrolysis) is suggestive of alkalinity or poor development of the soil (Retallack, 1990a). The increase in the ratio of silica to sesquioxides is related to a scarcity of hydrated minerals (Fig. 2).

Sedimentary zeolites are considered authigenic minerals, formed under saline and alkaline soil or lake settings (e.g., Hay, 1981; Gude and Sheppard, 1986; Retallack, 1990a; Renaut, 1993). The presence of abundant volcanic glass and plagioclase favors zeolite authigenesis, although these features are not considered an essential factor (Renaut, 1993). Following Hall (1998), it is considered that reworking of pyroclastic detritus in a lacustrine environment and subsequent pedogenesis in an alkaline soil environment probably is responsible for zeolite authigenesis in the Gran Salitral Formation.

Ichnology

The insect trace fossil association found in the calcareous paleosols of the Gran Salitral Formation is similar to that recorded from the Mercedes Formation of Uruguay (Martínez et al., 1997). Specimens of *Celliforma* are similar not only in general aspect but also in the arrangement of cells in rows. Moreover, the material mentioned and illustrated by Frenguelli (1930, 1938a,) from the Mercedes Formation and the material described herein includes one of the largest and one of the smallest specimens of *Celliforma* known. These ichnological similarities are also accompanied by the preservation of continental snails and ovoid structures in paleosols from both deposits. In contrast, the hackberry endocarps found in Uruguay were not recorded in La Pampa, although many kilometers of outcrops are still unexamined. It is also noteworthy that the *Teisseirei barattinia* recognized in the current study is absent in the Mercedes Formation. This ichnotaxon is recorded for the first time outside the typical Chacoparanense region (i.e., Uruguay and the neighboring Entre Ríos province in Argentina). This expands its regional importance although its biochron seems to be restricted to the Late Cretaceous-Oligocene interval (cf. Genise et al., 2000).

Calcareous paleosols recorded from United States and Kenya (Retallack, 1984; Thackray, 1994), apart from shells of continental snails and hackberry endocarps, contain similar fossil bee nests, which, in turn, are different from the clustered type described herein. This fact could reflect the predominance of different types of nest architecture in the Halictinae (the possible trace makers for all mentioned cases), inhabiting the northern and southern Hemispheres. In North America and Africa, the nests are composed of cells directly attached to main tunnels, a common design for nests of the cosmopolitan tribe Halictini. In contrast, the clustering of cells, like that of *Rosellichnus* isp., is more common in the neotropical Augochlorini (Eickwort and Sakagami, 1979). Similar bee traces encountered in two different South American paleosols suggest the existence of bees (halictines?) that preferred calcareous, alkaline soils to nest, an observation apparently not recorded in the literature of modern bees. Sakagami and Michener (1962) noted that, for the Halictinae, chemical and pedological properties of soils seemed to be of little importance in the process of selecting a nesting site. Cane (1992) analyzed soil texture and moisture where bees nest, pointing out that there were no studies for other soil properties. Rozen (1964) recorded the only bee, *Svastra obliqua* (Anthophorinae), known to nest in salt flats. In terms of bee diversity, it is possible to identify at least three species in the paleosols of La Pampa, each one constructing a different nesting trace. Nonetheless, this number may be higher if the dispersion of cell sizes included in both ichnospecies of *Celliforma* is considered. At least in *Celliforma roselli*, the two largest specimens probably belong to one species of bee, while the smaller specimens (30 mm in length and 15 mm in diameter) seem to belong to another species. The trace maker of *Rosellichnus* isp. could have been an Augochlorini (as suggested by cell morphology, size, and thin walls), whereas that of *C. germanica* may have been another species of sweat bee, possibly from the Agapostemonini (cf. Roberts, 1969; Abrams and Eickwort, 1980); both taxa are well represented in the Neotropical region at present.

The remaining invertebrate trace fossils convey little information about paleoenvironmental conditions and trace makers. *Skolithos* has been reported from a wide variety of environments, both marine and continental (e.g., Fillion and Pickerill, 1990). Dense groupings of *Skolithos* in continental settings (like that within paleosol 1) have been recognized in fluvial channel facies and point bars (Fitzgerald and Barrett, 1986; Woolfe, 1990; Buatois and Mángano, 1996). This ichnotaxon is interpreted as a dwelling burrow probably produced by an arthropod (cf. Ratcliffe and Fagerstrom, 1980; Fitzgerald and Barrett, 1986). In the present study, periodic fluctuation of the water table is considered to have been a critical factor for the occurrence of dense groupings of *Skolithos* (cf. Fitzgerald and Barrett, 1986). *Taenidium barretti* is recorded only from continental facies (Keighley and Pickerill, 1994). Different organisms have been suggested as producers of *Taenidium* (Buatois and Mángano, 1996), although the environmental setting and diameter of the described specimens probably restrict the potential trace makers to annelids (earthworms?) and arthropods.

The association of fossil bee cells in paleosols, like that described herein for paleosols 2 and 3, is taken as indica-

TABLE 2—Comparison of fundamental features for four known ichnological associations of insect trace fossils in calcareous paleosols.

Unit (location)	Mercedes (Uruguay)	Gran Salitral (Argentina)	Brule (South Dakota)	Higewi (Kenya)
Soil horizons	Cca?	Bw-C	A1-A2-A3-B2irt-B3ir-Cca	A-A/C-C
Parent material	Quartz sandstone	Reworked intermediate pyroclastic material	Reworked volcanic ash fall and alluvium	Reworked carbonatitic volcanic ash
Soil development	Moderate	Weak	Strong	Weak
Soil type		Inceptisol	Petrocalcic Palustalf	
Age	Paleocene	Early Eocene	Early Late Oligocene	Early–Middle Miocene
Insect trace fossils	*Celliforma germanica, Celliforma roselli*(?)	*Celliforma germanica, Celliforma roselli, Roselichnus* isp., *Teisseirei barattinia,* ovoid structures	*Celliforma ficoides, Pallichnus dakotensis*	*Celliforma habari,* cocoons
Associated ichnofossils	Rhizoliths	Root traces, *Skolithos linearis, Taenidium barretti,* unnamed burrow fillings	Various root traces	Root traces, burrows
Bee tribe	Augochlorini	Augochlorini, Agapostemonini	Halictini	Halictini
Associated fossils	Hackberry endocarps, terrestrial snails	Freshwater and terrestrial snails, notoungulate bones, herbaceous remains	Hackberry endocarps, terrestrial snail, vertebrate bones	Hackberry endocarps, terrestrial snails, grass leaves
Vegetation	Trees (*Celtis*)	Saltbush and sage (low vegetation)	Gallery woodland + savanna (*Celtis*)	Savanna + dry forest
Paleoclimate	Warm, arid	Warm, semiarid	Seasonal dry or cool, subhumid, sutropical to warm temperate	Humid–subhumid
Source	Martínez et al. (1997), Veroslavsky et al. (1997)	This paper	Retallack (1984)	Thackray (1989, 1994)

tive of open herbaceous paleoenvironments, considering that soil-nesting bees commonly prefer well-drained ground, that is exposed to solar radiation (Genise and Bown, 1994; Genise et al., 2000). In addition, the other insect trace fossil occurring at the Gran Salitral Formation, *Teisseirei barattinia*, is associated with bee and dung-beetle trace fossils in the type locality (Genise and Laza, 1998), suggesting a similar environment. The absence of dung-beetle trace fossils might indicate sparse plant coverage, such as that found within xeromorphic shrublands, which is consistent with the gastropod association, salinity and alkalinity indicators, and lack of extensive rooting.

A comparison with the other three known occurrences of the association of bee nests and continental gastropods in calcareous paleosols from Uruguay, Kenya, and the USA (Table 2), allows for the identification of some shared features. These include: (1) parent material commonly composed of reworked pyroclastic material; (2) colonization by sweat bees, which were important agents in the modification of the sedimentary fabric; (3) moderate alkalinity and, in some cases, also salinity; (4) association with low vegetation; and (5) development under warm, semiarid to subhumid climate.

A similar occurrence of palustrine facies, probable insect ichnofossils, and terrestrial and freshwater snails also is known from the late Eocene Bembridge Limestone of England (Edwards et al., 1998). In that deposit, the trace fossil association (whose taxonomy is still unresolved) is restricted to ovoid-cylindrical casts of chambers possibly constructed by insects for pupation or by other animals for aestivation or hibernation (Edwards et al., 1998). The trace fossil association described in the current paper also differs significantly from that typical of continental evaporite sequences described by Rodríguez-Aranda and Calvo (1998), especially with regard to the absence of hymenopterous nests in the latter.

Genise et al. (2000) suggested that associations of different types of bee cells, probable wasp cocoons (ovoid structures), and dung-beetle pupal chambers in calcareous paleosols be considered as a potentially separate ichnofacies. The new data presented herein add another occurrence of this potential ichnofacies, as well as the inclusion of *Teisseirei*. Additionally, this report broadens the range of environmental settings in which the association is found to include palustrine facies. At present, the association described herein can be provisionally included in the *Coprinisphaera* ichnofacies (Genise et al., 2000). Comparisons with other continental and lacustrine ichnofacies are not considered necessary due to the large differences with the described ichnologic association (cf. Buatois et al., 1998).

Gastropod Fauna

The ability of the extant Ampullariidae (which includes *Pomacea*) to withstand periods of desiccation and slight changes in salinity, and its general distribution in temperate to subtropical areas of Argentina, are in agreement with the general paleoenvironmental setting as deduced from sedimentological criteria. The association of the land snails *Plagiodontes* spp., *Bostryx* sp., and *Bulimulus* sp. indicates an environment similar to that found at present in the central-western provinces of Argentina, related to the Sierras Pampeanas, and particularly the Monte biogeographic region of Argentina (Cabrera and Willink, 1973).

The later is characterized by a subtropical to temperate climate dominated by xeric vegetation, similar to that of the xeromorphic shrublands (Mueller-Dombois and Ellenberg, 1980).

Vegetation

Insight about the vegetation that supported the Eocene paleosols come from micro- and macrofeatures and geochemical data. Alveolar and fenestral structures (0.2 to 2 mm in diameter) are interpreted as rootlet tubules filled by sparry calcite and occasionally by microlaminated clay, which were formed very early during diagenesis (cf. Mount and Cohen, 1984; Wright et al., 1988; Alonso-Zarza et al., 1992). Paleosol 3 supported sparse herbaceous plants (as suggested by relatively abundant, fine alveolar structure and root traces in its cambic horizon, Fig. 3E), as well as rare medium-sized trees or shrubs. Hence, lake mudflats probably were covered by sparse, low vegetation like saltbush and sage.

The Cerling model for carbon isotopic composition of soil carbonates (e.g., Cerling, 1984; Cerling and Quade, 1993) is not applicable to the Gran Salitral palustrine paleosols because its matrix was not leached of calcium carbonate (T. Cerling, pers. commun., 2001). The complications imposed by uncertainties about isotopic composition, CO_2 concentration of the atmosphere, and the discrimination by plants impedes the estimation of the proportion of pedogenic carbonates in palustrine samples following the methodology of Magaritz and Amiel (1980).

Paleoclimate

The presence of abundant hymenopterous nests and sparse vegetation reinforce xeric conditions as determined from other geologic data. The association of incipient surface karst with relatively thick calcareous paleosols, as those described in this paper, is linked to carbonate parent material that has been exposed to meteoric diagenesis under a semiarid and warm climate (James and Choquette, 1990). Precipitation of evaporites (former evaporite nodules replaced by length-slow chalcedony and gypsum laminae) also is indicative of semiarid conditions, at least in part of the sequence. The low values of the chemical index of alteration (CIA; from 42 to 64) are equivalent to fresh or mildly weathered intermediate igneous rocks (cf. Nesbitt and Young, 1982) and also suggest that the availability of water was restricted during weathering. Furthermore, the development of clotted-peloidal structure requires variation in the availability of water during the year and hence is related to seasonal climate (e.g., Freytet and Plaziat, 1982; Platt, 1989; Armenteros and Daley, 1998).

The $\delta^{18}O$ of pedogenic carbonate is in equilibrium with palustrine/soil water, whose isotopic composition is related to meteoric water, although there are various complicating factors that are not understood completely (Cerling and Quade, 1993). Some authors (e.g., Suchecki et al., 1988; Quade et al., 1995; Yemane and Kelts, 1996) have used absolute $\delta^{18}O$ values of pedogenic carbonate to estimate paleotemperature, although this practice is preliminary (Cerling and Quade, 1993). Mean annual temperature for paleosol 3 was estimated using the equation of Hays and Grossmann (1991) for inland recharge, and assuming $\delta^{18}O$ for Paleogene seawater of -1 ‰ SMOW (Shackleton and Kennett, 1975). The equation for coastal recharge of Hays and Grossman (1991) is more suitable, given the early Eocene paleogeographic setting for the study area (Franchi et al., 1984). Among the solutions for that equation, which are 0°C and 26°C, the lower temperature estimate is rejected because it conflicts with the sedimentological and faunal evidence that supports a temperate-warm climate. The approximation of 26°C corresponds to average soil temperature at about 1 m depth where carbonate forms, which is 2–3°C above the mean annual air temperature (cf. Quade et al., 1995). An air temperature estimate of 23°C – 24°C agrees with warm climatic conditions characteristic of palustrine carbonates, as well as with the general view that the early Eocene was a time of global warmth and reduced latitudinal temperature gradients compared with the present day (e.g., Zachos et al.; 1994 Greenwood and Wing, 1995; Sloan and Rea, 1995).

CONCLUSIONS

Early Eocene calcareous paleosols from La Pampa province (Argentina) developed on lake-margin, carbonate-dominated deposits subject to repeated flooding and desiccation. Short (annual?) and long-term water-level fluctuations under warm, seasonal climate favored the development of distinctive palustrine features. However, paleosols are not fully developed because of prevailing semiarid conditions. The succession contains a moderately diverse insect ichnofauna (*Celliforma*, *Rosellichnus*, *Teisseirei*, and probably ovoid structures), few plant ichnofossils, and other animal trace fossils of uncertain origin. Remarkable features of the Gran Salitral ichnofauna are the abundance of bee nests; apparent preference for calcareous, alkaline and mildly saline soils in a playa-like setting; and association with low and sparse vegetation. The documentation of this insect-dominated ichnologic association from calcareous paleosols strengthens the cause for distinguishing a new continental ichnofacies (cf. Genise et al., 2000) with particular environmental implications, although further studies are needed.

ACKNOWLEDGMENTS

Preliminary observations on the ichnology and sedimentology of the Gran Salitral Formation were made as part of mapping work for the Servicio Nacional de Geología y Minería of Argentina under contract with the Universidad Nacional de La Pampa. Néstor Sandoval kindly conducted part of the photographic artwork for this article. Lora Wingate (Stable Isotopes Laboratory, University of Michigan, Ann Arbor) patiently analyzed the C and O isotopic composition of samples for this study. Thure Cerling is thanked for his comments on the stable isotopic data.

REFERENCES

ABRAMS, J., and EICKWORT, G.C., 1980, Biology of the communal sweat bee *Agapostemon virescens* (Hymenoptera: Halictidae) in New York state: Research Agriculture, Cornell University Agricultural Experiment Station, v. 1, p. 1–20.

ALLAN, J.R., and MATTHEWS, R.K., 1982, Isotopic signatures associ-

ated with early meteoric diagenesis: Sedimentology, v. 29, p. 797–817.

ALONSO-ZARZA, A.M., and CALVO, J.P., 2000, Palustrine sedimentation in an episodically subsiding basin: The Miocene of the northern Teruel Graben (Spain): Palaeogeography, Palaeoclimatology, Palaeoecology, v. 160, p. 1–21.

ALONSO-ZARZA, A.M., CALVO, J.P., and GARCÍA DEL CURA, M.A., 1992, Palustrine sedimentation and associated features—grainification and pseudo-microkarst—in the Middle Miocene (Intermediate Unit) of the Madrid Basin, Spain: Sedimentary Geology, v. 73, p. 43–61.

ARMENTEROS, I., and DALEY, B., 1998, Pedogenic modification and structure evolution in palustrine facies as exemplified by the Bembridge Limestone (Late Eocene) of the Isle of Wight, southern England: Sedimentary Geology, v. 119, p. 275–295.

ARMENTEROS, I., RECIO, C., and DALEY, D., 1992. Sedimentology and stable isotope study of the lacustrine Bembridge Limestone (Upper Eocene), Isle of Wight, Southern England: III Congreso Geológico de España and VIII Congreso Latinoamericano de Geología, Salamanca, Simposios 1, p. 27–38.

BEIER, J.A., 1987, Petrographic and geochemical analysis of caliche profiles in a Bahamian Pleistocene dune: Sedimentology, v. 34, p. 991–998.

BOWN, T.M., HASIOTIS, S.T., GENISE, J F., MALDONADO, F., and BROUWERS, E.M., 1997, Trace fossils of Hymenoptera and other insects and paleonvironments of the Claron Formation (Paleocene and Eocene), Southwestern Utah: United States Geological Survey Bulletin 2153, p. 42–58.

BUATOIS, L.A., and MÁNGANO, M.G., 1996, Icnología de ambientes continentales: Problemas y perspectivas: Asociación Paleontológica Argentina, Publicación Especial v. 4, p. 5–30.

BUATOIS, L.A., MÁNGANO, M.G., GENISE, J.F., and TAYLOR, T.N., 1998, The ichnologic record of the invertebrate invasion of nonmarine ecosystems: Evolutionary trends in ecospace utilization, environmental expansion, and behavioral complexity: PALAIOS, v. 13, p. 217–240.

BULLOCK, P., FEDOROFF, N., JONGERIUS, A., STOOPS, G., TURSINA, T., and BABEL, U., 1985, Handbook of Soil Thin Section Description: Waine Research Publications, Wolverhampton, 152 p.

BUOL, S.W., HOLE, F.D., and MCCRACKEN, R.J., 1990, Génesis y Clasificación de Suelos, 2nd edition: Editorial Trillas, México, 417 p.

CABRERA, A.L., and WILLINK, A., 1973, Biogeografía de América Latina: Editorial Secretaría General de la Organización de Estados Americanos, Monografías Científicas, Serie Biología, Washington, v. 13, 120 p.

CANE, J.H., 1992, Soils of ground-nesting bees (Hymenoptera: Apoidea): Texture, moisture, cell depth and climate: Journal of Kansas Entomological Society, v. 64, p. 406–413.

CASTELLANOS, Z.J., and FERNÁNDEZ, D., 1976, Ampullaridae: Fauna de Agua Dulce de la República Argentina, v. 15, p. 1–33.

CERLING, T.E., 1984, The stable isotopic composition of modern soil carbonate and its relationship to climate: Earth and Planetary Science Letters, v. 71, p. 229–240.

CERLING, T.E., and QUADE, J., 1993, Stable carbon and oxygen isotopes in soil carbonates: *in* Swart, P.K., Lohmann, K.C., McKenzie, J., and Savin, S., eds., Climate Change in Continental Isotopic Records: American Geophysical Union, Geophysical Monograph 78, p. 217–231.

CERLING, T.E., BOWMAN, J.R., and O'NEIL, J.R., 1988, An isotopic study of a fluvial-lacustrine sequence: The Plio-Pleistocene Koobi Fora sequence, East Africa: Palaeogeography, Palaeoclimatology, Palaeoecology, v. 63, p. 335–356.

EDWARDS, N., JARZEMBOWSKI, E.A., PAIN, T., and DALEY, B., 1998, Cocoon-like trace fossils from the lacustrine-palustrine Bembridge Limestone Formation (Late Eocene), Southern England: Proceedings of the Geologists Association, v. 109, p. 25–32.

EICKWORT, G.C., and SAKAGAMI, S.F., 1979, A classification of nest architecture of bees in the tribe Augochlorini (Hymenoptera: Halictidae: Halictinae) with description of a Brazilian nest of *Rhinocorynura inflaticeps*: Biotropica, v. 11, p. 28–37.

ESTEBAN, M., and KLAPPA, C.F., 1983, Subaerial exposure environment: *in* Scholle, P.A., Bebout, D.G., and Moore, C.H., eds., Carbonate Depositional Environments: American Association of Petroleum Geologists, Memoir 33, p. 1–63.

EUGSTER, H.P., and KELTS, K., 1983, Lacustrine chemical sediments: *in* Goudie, A.S., and Pye, K., eds., Chemical Sediments and Geomorphology: Academic Press, London, p. 321–368.

FANNING, D.S., and FANNING, M.C.B., 1989, Soil: Morphology, Genesis, and Classification: John Wiley & Sons, New York, 395 p.

FEDO, C.M., NESBITT, H.W., and YOUNG, G.M., 1995, Unraveling the effects of potassium metasomatism in sedimentary rocks and paleosols, with implications for paleoweathering conditions and provenance: Geology, v. 23, p. 921–924.

FENTON, T.E., 1983, Mollisols: *in* Wilding, L.P., Smeck, N.E., and Hall, G.F., eds., Pedogenesis and Soil Taxonomy. II. The Soil Orders, Developments in Soil Science: Elsevier, Amsterdam, v. 11B, p. 125–163.

FERNÁNDEZ, D., 1973, Catálogo de la malacofauna terrestre argentina: Monografías de la Comisión de Investigaciones Científicas de la provincia de Buenos Aires, v. 4, p. 1–197.

FILLION, D., and PICKERILL, R.K, 1990, Ichnology of the Upper Cambrian? To Lower Ordovician Bell Island and Wabana groups of eastern Newfoundland, Canada: Palaeontographica Canadiana, v. 7, p. 1–119.

FITZGERALD, P.G., and BARRETT, P.J., 1986, *Skolithos* in a Permian braided river deposit, southern Victoria Land, Antarctica: Palaeogeography, Palaeoclimatology, Palaeoecology, v. 52, p. 237–247.

FOSS, J.E., MOORMANN, F.R., and RIEGER, S., 1983, Inceptisols: *in* Wilding, L.P., Smeck, N.E., and Hall, G.F., eds., Pedogenesis and Soil Taxonomy. II. The Soil Orders, Developments in Soil Science: Elsevier, Amsterdam, v. 11B, p. 355–381.

FRANCHI, M.R., NULLO, F., SEPÚLVEDA, E., and ULIANA, M.A., 1984, Las sedimentitas terciarias: *in* Relatorio 9° Congreso Geológico Argentino, San Carlos de Bariloche, p. 215–266.

FRENGUELLI, J., 1930, Apuntes de geología uruguaya: Boletín del Instituto de Geología y Perforaciones (Uruguay), v. 11, p. 1–47.

FRENGUELLI, J., 1938a, Bolas de escarabeidos y nidos de véspidos fósiles: Physis, v. 12, p. 348–352.

FRENGUELLI, J., 1938b, Nidi fossili di Scarabeidi e Vespidi: Bolletino Societta Geologia Italiana, v. 57, p. 77–96.

FREYTET, P., 1973, Petrography and paleoenvironment of carbonated continental deposits with particular reference to the Upper Cretaceous and Lower Eocene of Languedoc (southern France): Sedimentary Geology, v. 10, p. 25–60.

FREYTET, P., 1984, Carbonate lacustrine sediments and their transformations by emersion and pedogenesis: Importance of identifying them for paleogeographical reconstructions: Bulletin Centres de Recherches et Exploration-Production Elf-Aquitainie, v. 8, p. 223–247.

FREYTET, P., and PLAZIAT, J.C., 1982, Continental carbonate sedimentation and pedogenesis—Late Cretaceous and early Tertiary of southern France: Contributions to Sedimentology, v. 12, p. 1–213.

GENISE, J.F., 2001, The ichnofamily Celliformidae for *Celliforma* and allied ichnogenera: Ichnos, v. 7, p. 267–282.

GENISE, J.F., and BOWN, T.M., 1994, New Miocene scarabeid and hymenopterous nests and Early Miocene (Santacrucian) paleoenvironments, Patagonian Argentina: Ichnos, v. 3, p. 107–117.

GENISE, J.F., and BOWN, T.M., 1996, *Uruguay* Roselli and *Roselli-chnus* n. ichnogen. two ichnogenera for cluster of fossil bee cells: Ichnos, v. 4, p. 199–217.

GENISE, J.F., and LAZA, J.H., 1998, *Monesichnus ameghinoi* Roselli: A complex insect trace fossil produced by two distinct trace makers: Ichnos, v. 5, p. 213–223.

GENISE, J.F., MÁNGANO, M.G., BUATOIS, L.A., LAZA, J.H., and VERDE, M., 2000, Insect trace fossils associations in paleosols: The *Coprinisphaera* ichnofacies: PALAIOS, v. 15, p. 49–64.

GODDARD, E.N., PARKER, T.D., DE FORD, R.K., ROVE, O.N., SINGEWALD, J.T., and OVERBECK, R.M., 1980, The Rock Color Chart: Geological Society of America, Boulder.

GOLDSTEIN, R.H., 1991, Stable isotope signatures associated with paleosols, Pennsylvanian Holder Formation, New Mexico: Sedimentology, v. 38, p. 67–77.

GREENWOOD, D.R., and WING, S.L., 1995, Eocene continental climates

and latitudinal temperature gradients: Geology, v. 23, p. 1044–1048.

GUDE, A.J., and SHEPPARD, R.A., 1986, Zeolitic diagenesis of tuffs in an Upper Miocene lacustrine deposits near Durkee, Baker County, Oregon: *in* Mumpton, F.A., ed., Studies in diagenesis: U.S. Geological Survey Bulletin 1578, p. 301–333.

HALL, A., 1998, Zeolitization of volcaniclastic sediments: The role of temperature and pH: Journal of Sedimentary Research, v. 68, p. 739–745.

HALLEY, R.B., 1977, Ooid fabric and fracture in the Great Salt Lake and the geological record: Journal of Sedimentary Petrology, v. 47, p. 1099–1120.

HAY, R.L., 1981, Geology of zeolites in sedimentary rocks: *in* Mumpton, F.A., ed., Mineralogy and Geology of Natural Zeolites: Mineralogical Society of America, Reviews in Mineralogy 4, p. 53–64.

HAYS, P.D., and GROSSMAN, E.L., 1991, Oxygen isotopes in meteoric calcite cements as indicators of continental paleoclimate: Geology, v. 19, p. 441–444.

HESS, R., 1990, Silica diagenesis: Origin of inorganic and replacement cherts: *in* McIlreath, I.A., and Morrow, D.W., eds., Diagenesis: Geoscience Canada, Reprint Series 4, p. 253–275.

JAMES, N.P., and CHOQUETTE, P.W., 1990, Limestones—The meteoric diagenetic environment: *in* McIlreath, I.A., and Morrow, D.W., eds., Diagenesis: Geoscience Canada, Reprint Series 4, p. 35–73.

KEIGHLEY, D.G., and PICKERILL, R.K., 1994, The ichnogenus *Beaconites* and its distinction from *Anchorichnus* and *Taenidium*: Palaeontology, v. 37, p. 305–337.

LINARES, E., LLAMBÍAS, E.J., and LATORRE, C.O., 1980, Geología de la Provincia de La Pampa, República Argentina y Geocronología de sus rocas metamórficas y eruptivas: Revista de la Asociación Geológica Argentina, v. 35, p. 87–146.

MAGARITZ, M., and AMIEL, A.J., 1980, Calcium carbonate in a calcareous soil from the Jordan Valley, Israel: Its origin as revealed by the stable carbon isotope method: Soil Science Society America Journal, v. 44, p. 1059–1062.

MARTÍNEZ, S., VEROSLAVSKY, G., and VERDE, M., 1997, Primer registro del Paleoceno en el Uruguay: Paleosuelos calcáreos fosilíferos en la Cuenca de Santa Lucía: Revista Brasileira de Geociencias, v. 27, p. 295–302.

MELCHOR, R.N., and CASADÍO, S.A., 2000, Descripción Geológica de la Hoja 3766-III "La Reforma" (1:250.000), Provincia de la Pampa: Boletín del Servicio Geológico Minero Argentino, v. 295, p. 1–56.

MILLIKEN, K.L., 1979, The silicified evaporite syndrome—Two aspects of silicification history of former evaporite nodules from southern Kentucky and northern Tennessee: Journal of Sedimentary Petrology, v. 49, p. 245–256.

MILROY, P.G., and WRIGHT, V.P., 2000, A highstand oolitic sequence and associated facies from a Late Triassic lake basin, south-west England: Sedimentology, v. 47, p. 187–209.

MOUNT, J.F., and COHEN, A.S., 1984, Petrology and geochemistry of rhizoliths from Plio-Pleistocene fluvial and marginal lacustrine deposits, east Lake Turkana, Kenya: Journal of Sedimentary Petrology, v. 54, p. 263–275.

MUELLER-DOMBOIS, D., and ELLENBERG, H., 1980, Aims and Methods of Vegetation Ecology: John Wiley & Sons, New York, 525 p.

NESBITT, H.W., and YOUNG, G.M., 1982, Early Proterozoic climate and plate motions inferred from major element chemistry of lutites: Nature, v. 299, p. 715–717.

PARODIZ, J.J., 1939, Revisión de *Plagiodontes* y *Scalarinella*: Physis, v. 17, p. 711–734.

PLATT, N.H., 1989, Lacustrine carbonates and pedogenesis: Sedimentology and origin of palustrine deposits from the Early Cretaceous Rupelo Formation, W Cameros Basin, N Spain: Sedimentology, v. 36, p. 665–680.

PLATT, N.H., and WRIGHT, V.P., 1991, Lacustrine carbonates: Facies models, facies distributions and hydrocarbon aspects: *in* Anadón, P., Cabrera, L., and Kelts, K., eds., Lacustrine Facies Analysis: International Association of Sedimentologists, Special Publication 13, p. 57–74.

PLATT, N.H., and WRIGHT, V.P., 1992, Palustrine carbonates and the Florida Everglades: Towards an exposure index for the fresh-water environment?: Journal of Sedimentary Petrology, v. 62, p. 1058–1071.

QUADE, J., CATER, J.L., OJHA, T.P., ADAM, J., and HARRISON, T.M., 1995, Late Miocene environmental change in Nepal and the northern Indian subcontinent: Stable isotopic evidence from paleosols: Geological Society of America Bulletin, v. 107, p. 1381–1397.

RATCLIFFE, B.C., and FAGERSTROM, J.A., 1980, Invertebrate lebensspuren of Holocene floodplains: Their morphology, origin, and ecological significance: Journal of Paleontology, v. 54, p. 614–630.

RENAUT, R.W., 1993, Zeolitic diagenesis of late Quaternary fluviolacustrine sediments and associated calcrete formation in the Lake Bogoria Basin, Kenya Rift Valley: Sedimentology, v. 40, p. 271–301.

RETALLACK, G.J., 1984, Trace fossils of burrowing beetles and bees in an Oligocene paleosol, Badlands National Park, South Dakota: Journal of Paleontology, v. 58, p. 571–592.

RETALLACK, G.J., 1990a, Soils of the Past—An Introduction to Paleopedology: Unwin Hyman, Boston, 520 p.

RETALLACK, G.J., 1990b, The work of dung beetles and its fossil record: *in* Boucot, A.J., ed., Evolutionary Paleobiology of Behavior and Coevolution: Elsevier, Amsterdam, p. 214–226.

RETALLACK, G.J., 1997, A Colour Guide to Paleosols: John Wiley & Sons, Chichester, 175 p.

RODRÍGUEZ-ARANDA, J.P., and CALVO, J.P., 1998, Trace fossils and rhizoliths as a tool for sedimentological and palaeoenvironmental analysis of ancient continental evaporite successions: Palaeogeography, Palaeoclimatology, Palaeoecology, v. 140, p. 383–399.

ROBERTS, R.B., 1969, Biology of the bee genus *Agapostemon* (Hymenoptera: Halictidae): The University of Kansas Science Bulletin, v. 48, p. 689–719.

ROSELLI, F.L., 1938, Apuntes de geología y paleontología uruguaya. Sobre insectos del Cretácico del Uruguay o descubrimiento de admirables instintos constructivos de esa época: Boletín de la Sociedad Amigos de las Ciencias Naturales "Kraglievich-Fontana", v. 1, p. 72–102.

ROSELLI, F.L., 1976, Contribución al estudio de la geopaleontología de los departamentos de Colonia y Soriano, Uruguay: Imprenta Cooperativa, Montevideo, 172 p.

ROSELLI, F.L., 1987, Paleoicnología: Nidos de insectos fósiles de la cobertura Mesozoica del Uruguay: Publicaciones del Museo Municipal de Nueva Palmira, v. 1, p. 1–56.

ROSSINSKY, V., and SWART, P.K., 1993, Influence of climate on the formation and isotopic composition of calcretes: *in* Swart, P.K., Lohmann, K.C., McKenzie, J., and Savin, S., eds., Climate Change in Continental Isotopic Records: American Geophysical Union, Geophysical Monograph 78, p. 67–75.

ROZEN, J.G., 1964, The biology of *Svastra obliqua* (Say), with a taxonomic description of its larvae (Apoidea, Anthophoridae): American Museum Novitates, v. 2170, p. 1–13.

SAKAGAMI, S.F., and MICHENER, C.D., 1962, The nest architecture of the sweat bees (Halictinae); a comparative study of behavior: University of Kansas Press, Lawrence, 135 p.

SCHÜTZE, E., 1907, Alttertiäre Land- und Süfswasserfossilien aus der Bunten Breccie von Weilheim im Riese: *in* Branca, W., and Fraas, E., eds., Die Lagerungsverhalttenisse Bunter Breccie an der Bahnlinie Donaukworth-Trreuchtlingen und ihre Bedeutung fur das Riesproblem: Physilakische Abhandlungen der Koniglich Preussischen Akademie der Wissenschaften, Berlin, v. 2, p. 25–26.

SHACKLETON, N.J., and KENNETT, J.P., 1975. Paleotemperature history of the Cenozoic and the initiation of the Antarctic glaciation: Oxygen and carbon isotope analyses in DSDP sites 277, 279, and 281: *in* Kennett, J.P., Houtz, R.E. et al., Initial Reports of the Deep Sea Drilling Project: U.S. Government Printing Office, Washington. D.C., v. 29, p. 743–755.

SLOAN, L.C., and REA, D.K., 1995, Atmospheric carbon dioxide and early Eocene climate: A general circulation modeling sensitivity study: Palaeogeography, Palaeoclimatology, Palaeoecology, v. 119, p. 275–292.

SOIL SURVEY STAFF, 1999, Soil taxonomy—A basic system of soil classification for making and interpreting soil surveys: United States Department of Agriculture, National Resources Conservation Service, Washington, Agriculture Handbook 436 (2nd edition), p. 1–870.

SUCHECKI, R.K., HUBERT, J.F., and DE WET, C.C.B., 1988, Isotopic imprint of climate and hydrogeochemistry on terrestrial strata of

the Triassic—Jurassic Hartford and Fundy rift basins: Journal of Sedimentary Petrology, v. 58, p. 801–811.

TALMA, A.S., and NETTERBERG, F., 1983, Stable isotope abundances in calcretes: *in* Wilson, R.C.L., ed., Residual Deposits: Geological Society of London, Special Publication 13, p. 221–233.

TANNER, L.H., 2000, Palustrine-lacustrine and alluvial facies of the (Norian) Owl Rock Formation (Chinle Group), Four Corners region, southwestern U.S.A.: Implications for Late Triassic paleoclimate: Journal of Sedimentary Research, v. 70, p. 1280–1289.

THACKRAY, G.D., 1989, Paleoenvironmental analysis of paleosols and associated fossils in Miocene volcaniclastic deposits, Rusinga Island, western Kenya: Unpublished Master of Science Thesis, University of Oregon, Eugene, 142 p.

THACKRAY, G.D., 1994, Fossil nest of sweat bees (Halictinae) from a Miocene paleosol, Rusinga Island, western Kenya: Journal of Paleontology, v. 68, p. 795–800.

VANSTONE, S.D., 1998, Late Dinantian palaeokarst of England and Wales: Implications for exposure surface development: Sedimentology, v. 45, p. 19–37.

VEROSLAVSKY, G., MARTÍNEZ, S., and DE SANTA ANA, H., 1997, Calcretas de aguas subterráneas y pedogénicas: Génesis de los depósitos carbonáticos de la Cuenca de Santa Lucía, sur del Uruguay (Cretácico Superior?—Paleógeno): Revista de la Asociación Argentina de Sedimentología, v. 4, p. 25–35.

WOOLFE, K.J., 1990, Trace fossils as paleoenvironmental indicators in the Taylor Group (Devonian) of Antarctica: Palaeogeography, Palaeoclimatology, Palaeoecology, v. 80, p. 301–310.

WRIGHT, V.P., and ALONSO-ZARZA, A.M., 1992, Significado de la composición isotópica ($\delta^{13}C$ y $\delta^{18}O$) en paleosuelos carbonatados. Mioceno de la Cuenca de Madrid: Geogaceta, v. 11, p. 61–63.

WRIGHT, V.P., PLATT, N.H., and WIMBLEDON, W. A., 1988, Biogenic laminar calcretes: Evidence of calcified root-mat horizons in paleosols: Sedimentology, v. 35, p. 603–620.

YEMANE, K., and KELTS, K., 1996, Isotope geochemistry of Upper Permian early diagenetic calcite concretions: Implications for Late Permian waters and surface temperatures in continental Gondwana: Palaeogeography, Palaeoclimatology, Palaeoecology, v. 125, p. 51–73.

ZACHOS, J.C., STOTT, L.D., and LOHMANN, K. C., 1994, Evolution of early Cenozoic marine temperatures: Paleoceanography, v. 9, p. 353–387.

ACCEPTED JULY 5, 2001

APPENDIX 1

Major oxides data.

	Sample ID						
	256A %	257A %	257B %	257C %	257D %	258A %	259A %
SiO_2	42.81	43.70	41.49	45.13	51.10	54.46	67.09
Al_2O_3	9.77	8.56	8.56	6.56	5.81	5.42	6.87
Fe_2O_3	2.45	2.30	2.13	1.81	1.66	1.50	1.83
FeO	−0.10	−0.10	−0.10	−0.10	−0.10	−0.10	−0.10
MnO	0.051	0.047	0.038	0.025	0.025	0.036	0.026
MgO	1.29	1.15	1.07	0.92	0.86	0.76	1.13
CaO	21.01	20.73	23.39	21.33	18.97	18.41	8.29
Na_2O	1.75	1.70	1.57	1.37	1.32	0.94	0.79
K_2O	1.44	1.29	1.20	0.96	0.96	0.76	0.99
TiO_2	0.315	0.295	0.279	0.233	0.202	0.180	0.204
P_2O_5	0.47	0.40	0.32	0.22	0.26	0.48	0.08
LOI	19.50	19.61	20.81	20.03	19.21	18.04	13.19
Total	100.76	99.68	100.76	98.49	100.28	100.89	100.39
CO_2	14.40	13.90	14.80	16.10	14.80	12.70	4.70
	ppm	ppm	ppm	ppm	ppm	ppm	ppm
Ba	605	484	196	140	337	321	66
Sr	787	1271	1042	791	793	945	838
Y	22	19	16	13	13	20	6
Sc	7	6	6	4	4	4	3
Zr	79	77	69	60	65	74	65
Be	−1	−1	−1	−1	−1	−1	−1
V	120	125	127	160	129	112	76

APPENDIX 2
Carbon and oxygen isotopic data from low-Mg calcite.

Sample ID	Lithology	$\delta^{13}C$ (‰ VPDB)	$\delta^{18}O$ (‰ VPDB)
256A	marl	−4.25	−5.54
256A	marl	−4.26	−5.46
256A	marl	−4.35	−5.69
256A	marl	−4.27	−5.81
257A	marl	−4.59	−3.15
257A	marl	−4.52	−3.16
257B	marl	−4.84	−3.03
257B	marl	−4.75	−3.07
257B	marl	−4.74	−3.07
257C	marl	−5.34	−3.47
257C	marl	−5.24	−3.48
257D	marl	−5.39	−3.49
257D	marl	−5.45	−3.40
257D	marl	−5.39	−3.51
257A	marl	−5.37	−3.30
258A	marl	−5.65	−3.25
259A	tuff	−5.38	−3.52
259A	tuff	−5.40	−3.49
259A*	50% matrix 50% spar	−5.71	−3.38
259A*	mostly sparry calcite	−6.76	−4.89
259A*	matrix	−5.59	−3.25
259A*	85% matrix	−5.37	−2.82
259A*	85% matrix	−5.46	−3.01
259A*	95% spar	−5.74	−3.58
259A*	95% spar	−6.01	−3.84
259A*	80% matrix	−6.08	−3.68
259A*	80% matrix	−5.71	−3.35
259A*	95% spar	−7.13	−5.51
259A*	85% matrix	−5.66	−3.05
259A*	85% matrix	−5.60	−3.09
259A*	90% matrix	−5.35	−2.78
259A*	95% spar	−6.65	−5.11
259A*	95% spar	−6.60	−4.92

* Material obtained by drilling on polished slab.

APPENDIX 3
Mineralogy from x-ray diffractrometry.

Sample ID	Lithology	Dominant mineral	Secondary minerals
256A	limestone	cal–plag	q–phi–zeo?
247A	marl	cal	phi–q–plag–k
257B	limestone	cal–plag	cli–zeo–q
257C	marl	cal–plag	q–mor–cli?
257D	marl	cal	mor–plag
258A	marl	cal	mor–zeo–sm
259A	tuff	q–cal	plag–mor–cli–phi?

cal: low-magnesium calcite, plag: plagioclase, k: potassium feldspar, q: quartz, zeo: unidentified zeolites; mor: mordenite; phi: phillipsite; cli: clinoptilolite; sm: smectite.

APPENDIX 4

Redescription of *Teisseirei*.

Teisseirei barattinia Roselli 1938
Figs. 12A, B, C, D, E, I

Teisseirei barattinia. Roselli, 1938, p. 82.
Tesseireichnus barattinia. Roselli, 1976, p. 167 (junior synonym).
Teisserichnus barattinia. Roselli, 1987, p. 24 (*lapsus*).
Teisseirichnus barratini. Retallack, 1990b, p. 219 (junior synonym).
Teisseirei barattinia. Genise and Laza, 1998, p. 213.

Holotype: MFLR 645. A complete specimen, broken in two pieces, illustrated in Roselli (187, fig. 5, p. 45). Paratypes: MFLR 645a and 645b. Complete specimens, illustrated in Roselli (1987, figs. 5a and 5b, p. 45).

Examined material; The types and 230 specimens collected in Nueva Palmira, Las Flores, Palmitas, Carmelo, Soriano, Paraje Molles and Paysandú, Uruguay (MACN-LI 825 to 876 and 890 to 926; MFLR 800 to 941). Twelve specimens collected in Colón (from the Late Cretaceous-Early Tertiary Puerto Unzué Formation), Entre Ríos, Argentina (MACN-LI 877 to 889) and 57 specimens collected in Gran Salitral, La Pampa, Argentina (GHUNLPam 12462-1/2; 12471-1/8; 12473-1/7; 12478-1/10 and MACN-LI 1266 to 1280, 1296 to 1309).

Type locality: Palacio Member of the Asencio Formation (Late Cretaceous-Early Tertiary), Nueva Palmira, Uruguay.
Emended diagnosis: Depressed chambers, slightly arched downwards (Figs. 12A, 12E), that may show an anterior small, rounded, antechamber (Fig. 13D). The inner surface displays, in the best preserved specimens, a distinct lining bearing small elliptical scratches oriented mostly longitudinally. Some specimens are surrounded by a thick wall of uncertain (concretionary?) origin.

Remarks: The depressed cross section along with the internal microrelief distinguishes this ichnotaxon from any other attributed to insects.

Description: These traces may be commonly found in the field showing three preservational variants. As empty or passively filled chambers found *in situ* in paleosols; as isolated, detached, "clasts" composed of the chamber fillings; or, as empty or filled chambers surrounded by a thick wall. The original of this wall is still uncertain, the trace maker may construct it, or it may be of diagenetic origin. Specimens from the Gran Salitral Formation occur mostly as detached chamber fillings with the exception of one specimen that was found *in situ*, oriented horizontally in the paleosol. Only one of the collected specimens preserved the antechamber. The length of the chambers ranges from 30 mm to 52 mm (mean = 40.20 mm, n = 50); the width ranges from 13 mm to 20 mm (mean = 16.98 mm, n = 50) and the height ranges from 9 mm to 15 mm (mean = 11.63 mm, n = 50). The average proportion height: width: length in 50 specimens is 1 : 1.5 : 3.5, which gives the trace its depressed aspect. The length is the parameter that shows more dispersion, the height and width being more conservative, a fact that suggests that the trace makers showed a great variation in body length but preserving similar width and height. The antechamber displays a less depressed aspect than the chamber, measuring 15 mm in length, 12 mm in width, and 11 mm in height. Three specimens (GHUNLPam 12473-3; 12462-1 and MACN-LI 1309) show remains of the microrelief composed of small, elliptical, parallel scratches (about 2 mm long), preserved as positive epirelief (Fig. 12I).

The Eocene specimens from La Pampa are indistinguishable from those of the type locality in shape, size, microrelief, and position in paleosol, leaving no doubts about their assignment to *T. barattinia*.